January 2016

Simultaneous real-time imaging of leading and lagging strand synthesis reveals the coordination dynamics of single replisomes

Karl E. Duderstadt
University of Groningen, Technical University of Munich, Max Planck Institute of Biochemistry

Hylkje J. Geertsema
University of Groningen

Sarah A. Stratmann
University of Groningen

Christiaan M. Punter
University of Groningen

Arkadiusz W. Kulczyk
Harvard Medical School, Boston

See next page for additional authors

Simultaneous real-time imaging of leading and lagging strand synthesis reveals the coordination dynamics of single replisomes

Abstract

The molecular machinery responsible for DNA replication, the replisome, must efficiently coordinate DNA unwinding with priming and synthesis to complete duplication of both strands. Due to the anti-parallel nature of DNA, the leading strand is copied continuously, while the lagging strand is produced by repeated cycles of priming, DNA looping, and Okazaki-fragment synthesis. Here, we report a multidimensional single-molecule approach to visualize this coordination in the bacteriophage T7 replisome by simultaneously monitoring the kinetics of loop growth and leading-strand synthesis. We show that loops in the lagging strand predominantly occur during priming and only infrequently support subsequent Okazaki-fragment synthesis. Fluorescence imaging reveals polymerases remaining bound to the lagging strand behind the replication fork, consistent with Okazaki-fragment synthesis behind and independent of the replication complex. Individual replisomes display both looping and pausing during priming, reconciling divergent models for the regulation of primer synthesis and revealing an underlying plasticity in replisome operation.

Keywords

imaging, leading, lagging, strand, synthesis, reveals, coordination, dynamics, single, simultaneous, replisomes, real-time

Disciplines

Medicine and Health Sciences

Publication Details

Duderstadt, K. E., Geertsema, H., Stratmann, S. A., Punter, C. M., Kulczyk, A. W., Richardson, C. C. & van Oijen, A. M. (2016). Simultaneous real-time imaging of leading and lagging strand synthesis reveals the coordination dynamics of single replisomes. Molecular Cell, 64 (6), 1035-1047.

Authors

Karl E. Duderstadt, Hylkje J. Geertsema, Sarah A. Stratmann, Christiaan M. Punter, Arkadiusz W. Kulczyk, Charles C. Richardson, and Antoine M. van Oijen

Title:

Simultaneous real-time imaging of leading and lagging strand synthesis reveals the coordination dynamics of single replisomes

Authors: Karl E. Duderstadt[1,2,3*], Hylkje J. Geertsema[1], Sarah A. Stratmann[1], Christiaan M. Punter[1], Arkadiusz W. Kulczyk[4], Charles C. Richardson[4], Antoine M. van Oijen[1,5*]

Affiliations:

[1]Zernike Institute for Advanced Materials and Centre for Synthetic Biology, University of Groningen, Groningen, The Netherlands

[2]Structure and Dynamics of Molecular Machines, Max Planck Institute of Biochemistry, Martinsried, Germany

[3]Physik Department, Technische Universität München, Garching, Germany

[4]Biological Chemistry and Molecular Pharmacology, Harvard Medical School, Boston, United States of America

[5]Centre for Medical & Molecular Bioscience, University of Wollongong, and Illawarra Health & Medical Research Institute, Wollongong, NSW 2522, Australia

*Correspondence to: Karl E. Duderstadt (duderstadt@biochem.mpg.de), Antoine M. van Oijen (vanoijen@uow.edu.au)

Contact Information:
Dr Karl Duderstadt
Structure and Dynamics of Molecular Machines
Max-Planck Institute of Biochemistry
Am Klopferspitz 18
82152 Martinsried,
Germany
Phone:+49-89-8578-3033
Email: duderstadt@biochem.mpg.de
Internet: http://www.biochem.mpg.de/duderstadt

Summary

The molecular machinery responsible for DNA replication, the replisome, must efficiently coordinate DNA unwinding with priming and synthesis to complete duplication of both strands. Due to the anti-parallel nature of DNA, the leading strand is copied continuously, while the lagging strand is produced by repeated cycles of priming, DNA looping, and Okazaki-fragment synthesis. Here, we report a multidimensional single-molecule approach to visualize this coordination in the bacteriophage T7 replisome by simultaneously monitoring the kinetics of loop growth and leading-strand synthesis. We show that loops in the lagging strand predominantly occur during priming and only infrequently support subsequent Okazaki-fragment synthesis. Fluorescence imaging reveals polymerases remaining bound to the lagging strand behind the replication fork, consistent with Okazaki-fragment synthesis behind and independent of the replication complex. Individual replisomes display both looping and pausing during priming, reconciling divergent models for the regulation of primer synthesis and revealing an underlying plasticity in replisome operation.

Introduction

To efficiently replicate DNA, replisomes must solve a directionality problem. Daughter-strand templates generated at the replication fork have opposing polarities, but polymerases can only synthesize in one direction. This geometry permits the leading-strand polymerase to synthesize continuously, while the lagging-strand polymerase is forced to restart at short intervals, extending RNA primers to produce Okazaki fragments (Kornberg and Baker, 1992; Okazaki et al., 1968). The textbook 'trombone model' (Alberts et al., 1983), proposed for prokaryotic systems, offers an elegant solution to this directionality problem. In this model, the formation of a replication loop reorients the lagging-strand polymerase so that both polymerases reside in the same complex and advance in parallel. As synthesis of the nascent Okazaki fragment proceeds, the double-stranded DNA (dsDNA) product of the lagging-strand DNA polymerase and the single-stranded DNA (ssDNA) product of the helicase contribute to the formation of a loop that grows until the next cycle of Okazaki-fragment synthesis is initiated. The dynamic and transient nature of replication loops has made their study challenging, with Electron Microscopy of cross-linked intermediates in the T4 and T7 systems providing the most compelling characterization (Chastain et al., 2003; Park et al., 1998). Recent single-molecule observations of replication have provided an alternative, real-time means of exploration, revealing the temporal regulation of looping and priming (Duderstadt et al., 2014; Hamdan et al., 2009; Manosas et al., 2009; Pandey et al., 2009). Nonetheless, the inability to directly observe and correlate multiple kinetic events across the replication machinery greatly limits mechanistic understanding of the coordination of synthesis on the two strands.

The replication machinery of T7 serves as an elegant model system to study the orchestration of enzymatic events during replication. While it contains only four unique proteins, the organization of the T7 replisome closely mimics that of more complex organisms (Hamdan and Richardson, 2009). At its core lies the T7 gene 4 protein (gp4), which assembles into a hexameric ring that displays both helicase and primase activity. Multiple copies of the T7 DNA polymerase, a 1:1 complex of the T7 gene 5 protein (gp5) and the *Escherichia coli* thioredoxin processivity factor, synthesize DNA on the unwound ssDNA. Finally, the T7 gene 2.5 ssDNA-binding protein (gp2.5) transiently coats exposed ssDNA to enhance the lagging-strand polymerase synthesis rate and aid coordination within the replisome (Hamdan and Richardson, 2009; Lee et al., 2002).

How the slow enzymatic steps of priming and polymerase loading take place on the lagging strand without causing loss of coordination with continuous leading-strand synthesis is a long-standing question in the field of replication, and several divergent models have been proposed based on various strands of experimental evidence (Corn et al., 2005; Dixon, 2009; Frick et al., 1999; Hamdan et al., 2009; Lee et al., 2002; Lee et al., 2006; Li and Marians, 2000; Manosas et al., 2009; Pandey et al., 2009; Swart and Griep, 1995; Tanner et al., 2008; Yuzhakov et al., 1999). One model postulates that priming pauses leading-strand synthesis (**Figure 1A**) to ensure that the events on each daughter strand remain synchronized (Lee et al., 2006). Another hypothesizes that leading-strand synthesis continues during primer production through the formation of a ss loop, known as a priming loop (Nelson et al., 2008), between the ssDNA-bound primase and helicase (**Figure 1B**). In this scenario, coordination between the two polymerases would require the lagging-strand DNA polymerase to be faster than the one on the leading strand to make up for the lost time during primer synthesis (Pandey et al., 2009). In these and other models, the hand-off of a completed RNA primer to the polymerase starts Okazaki-fragment synthesis on the lagging strand and leads to the formation of an ss-ds loop, or replication loop (**Figure 1C**).

Recent work has further complicated our understanding of the molecular events during replication by demonstrating rapid polymerase exchange (Geertsema et al., 2014; Loparo et al., 2011) and the presence of more than two polymerases at the replication fork (Geertsema et al., 2014; McInerney et al., 2007; Reyes-Lamothe et al., 2010) supporting multiple simultaneous rounds of lagging-strand synthesis. Current models of replication have been unsuccessful in reconciling these and other disparate experimental observations, leaving the mechanism of coordination of daughter-strand synthesis unresolved. The broad diversity of observed replisome behaviors suggests an underlying plasticity that may be an intrinsic feature of replisome function. Methodologies that provide more detailed information about how the events on each daughter strand are correlated are required to clarify the enzymatic pathways exploited by the replisome.

To obtain kinetic detail on coordination between the two daughter strands, we developed an assay to simultaneously monitor the kinetics of leading-strand synthesis and lagging-strand loop formation by single replisomes. In contrast to past studies (Hamdan et al., 2009; Lee et al., 2006), our assay reveals two loop growth populations: ss loops, formed during priming, and ss-ds loops, formed when both the leading strand and Okazaki

fragment are synthesized simultaneously. While most looping events are paired with highly processive leading-strand synthesis, pausing coincident with priming is also observed. Strikingly, while ss looping events are frequent, occurring multiple times during each replication cycle, ss-ds loops are rare. Using single-molecule fluorescence experiments that visualize how individual DNA polymerases are spatially and temporally distributed in and around the replisome, we show that polymerases remain bound to the lagging strand behind the replication fork, consistent with Okazaki-fragment synthesis behind and independent of the replication complex. Taken together, our findings provide a picture of a highly dynamic replisome: continuously changing its composition and operating mode so that different reaction pathways can be accessed to ensure rapid and robust replication.

Results

Visualization of leading-strand synthesis

Single-molecule studies of DNA replication using fluorescence microscopy or force spectroscopy allow for the direct observation of distinct structural and kinetic states visited by replisomes. Existing methods, however, provide only a single observable of replication fork progression, such as the amount of DNA synthesized (Lee et al., 2006; Tanner et al., 2009; Yao et al., 2009) or the formation of loops (Hamdan et al., 2009; Manosas et al., 2009; Pandey et al., 2009). Such a one-dimensional readout limits the processes that can be studied, typically requiring simplified experimental conditions with some replisome components removed and only leading-strand synthesis supported (Lee et al., 2006; Manosas et al., 2009; Pandey et al., 2009; Syed et al., 2014; Tanner et al., 2008). Fully coordinated replication results in the simultaneous conversion of a single parental DNA molecule into two daughter DNA molecules, so there is a need for assays that reveal the dynamic coordination and relative kinetics on the leading and lagging strands.

To overcome the limitations of past approaches, we present here a method to simultaneously monitor synthesis rates on the leading and lagging strands. To this end, we engineered a replication fork into 48.5-kilobase (kb) long λ phage DNA molecules (Supplemental Experimental Procedures) with 14.8 kb of DNA ahead of the fork as parental replication template and 33.7 kb attached to the leading-strand arm (**Figure 2A**). DNA molecules were attached through the lagging-strand end of the fork to the bottom surface of a flow cell (**Figure 2B** and **Video S1**) and 1-μm beads were attached to the two arms to visualize length changes. A constant laminar flow applied to the flow cell results in a drag on the two beads that stretches the DNA molecules with a combined force of 2 pN

(Supplemental Experimental Procedures), a force low enough not to inhibit loop formation and replication kinetics (Hamdan et al., 2009). Since the beads successfully bind to only a fraction of the DNA ends, most replication substrates remain singly labeled with only a small subpopulation containing a bead attached to each end. Fortunately, the use of ultra-wide-field, low-magnification imaging allowed us to visualize tens of thousands of beads within one experiment (**Figure 2A**), without sacrificing resolution (**Figure S1**), providing sufficient throughput to offset the low yields of bead attachment. Rates obtained for leading-strand synthesis (105 ±19 bp·s^{-1}) under conditions excluding gp2.5 and priming (by omission of ribonucleotides; rNTPs) were consistent with past observations (Lee et al., 2006; Loparo et al., 2011; Pandey et al., 2009), confirming functional assembly of the replication substrate and proper attachment of the beads (**Figure S2 & Video S2**).

Expected outcomes for different mechanisms

Several models have been put forward to explain how slow enzymatic steps on the lagging strand can occur without loss of coordination with continuous leading-strand synthesis. However, to date, distinguishing between these models has been difficult due to the challenge of directly correlating kinetic events between the daughter strands. The assay presented here provides direct observations of kinetic events on each daughter strand, allowing for discrimination among mechanisms. To elucidate the power of two-channel, single-molecule observations of replication, and provide insight into the types of kinetic information available from these types of observations, we first consider the expected experimental outcomes for different mechanisms.

In coordinated replication, different operational modes of the replisome give rise to distinct bead kinetics (**Figure 3A**). During leading-strand synthesis and in the absence of loop formation, the length of the leading-strand arm increases, and ss template for the lagging strand emerges from the helicase. In the presence of a saturating concentration of gp2.5, which is required for coordinated replication (Lee et al., 2002), ssDNA is equal in length to dsDNA (Hamdan et al., 2009) (**Figure S3**). As a consequence, the position of the parental-strand bead (A) remains relatively constant, while the leading-strand bead (B) moves downstream with a rate approximately twice the rate of leading-strand synthesis—with equal contributions from the newly synthesized duplex DNA and the gp2.5-extended lagging strand (**Figure 3A; first panel**). When a priming site is recognized by the replisome, and primer synthesis is initiated, distinct outcomes are predicted for different models. If primer synthesis causes leading-strand synthesis to pause, both beads should

remain stationary (**Figure 3A; second panel**), whereas if leading-strand synthesis continues during priming, the two beads will move in opposite directions at the rate of leading-strand synthesis as an ss loop forms (**Figure 3A; third panel**).

Following priming, the loading of a lagging-strand polymerase onto the new primer is predicted to result in ss-ds loop formation. Since the DNA substrate is attached to the surface by the end of the lagging strand, ss-ds loop formation events pull both beads toward the attachment point. However, for the leading-strand bead (B) this shortening in length is countered by an increase in length from synthesis by the leading-strand polymerase; this results in an observed motion of the leading-strand bead (B) that is the difference between the leading- and lagging-strand polymerase synthesis rates. In contrast, the observed motion of the parental-strand bead (A) is the sum of the synthesis rates (**Figure 3A; fourth panel**).

Thus, the predicted bead kinetics for various models result in different outcomes (**Figure S4B,C, D**), demonstrating the wealth of information that can be obtained from the assay. One other convenient property of the experimental design is easy removal of all looping dynamics from the leading-strand synthesis traces simply by subtracting the motion of parental-strand bead (A) from that of leading-strand bead (B). This analysis allows for the kinetics on the leading and lagging strands to be clearly distinguished and modeled.

Simultaneous Imaging of DNA looping and Leading-Strand Synthesis

Observation of replication by single T7 replisomes reveals highly processive leading-strand synthesis correlated with multiple cycles of loop growth and release on the lagging strand. **Figure 3B** shows length changes in an individual DNA molecule as a function of time in the flow of a buffer containing gp4, gp5-trx, gp2.5, Mg^{2+}, four deoxynucleoside 5'-triphosphates, ATP and CTP – the subset of ribonucleoside triphosphates required for primase activity by gp4 (Frick et al., 1999; Scherzinger et al., 1977). Surprisingly, loop formation events start simultaneously with the initiation of leading-strand synthesis, a time at which limited lagging-strand template is available, and they occur continuously until the leading strand is completely duplicated. Rate reductions that coincide with loop formation events are observed in the leading-strand bead B trace, as compared to the corrected leading-strand trace (bead B – bead A).

To interpret the observed bead behavior, we considered the expected traces for the coordination models (**Figure S4B, C, D**). The pausing model predicts stalling events in both A and B traces prior to loop formation, a phenomenon not visible for the traces shown here (additional traces can be seen in **Figure S5**). In contrast, the ss-loop model predicts a slowing of leading-strand bead (B) motion during ss-loop growth (**Figure S4C, D**), consistent with the observed rate reductions (**Figure 3B**, traces 'B' versus 'B-A'). However, subsequent to these slowing events the ss-loop model predicts a pause or reversal in leading-strand bead (B) motion during ss-ds-loop growth (given a lagging-strand rate that is equal to or greater than the leading-strand rate, respectively). Strikingly, neither of these behaviors is observed, suggesting alternative possibilities: that ss-ds loops are too short lived to be apparent in the traces, that the lagging-strand synthesis rate is much lower than the leading-strand rate, or that ss-ds loops are not present.

To distinguish among the alternate mechanistic interpretations, we used an unbiased, quantitative analysis of the bead kinetics to identify different operational modes of the replisome. Past studies relied on manual identification of changes in bead kinetics resulting from polymerase synthesis (Lee et al., 2006; Tanner et al., 2008), loop growth (Hamdan et al., 2009), or pausing events (Lee et al., 2006); but two-bead observations of coordinated replication display a higher level of complexity, reflecting a combination of multiple behaviors. Furthermore, background noise due to random bead fluctuations, which obscures the transitions between kinetic states, is more pronounced at the low forces required to avoid inhibition of loop formation (Hamdan et al., 2009). To detect kinetic changes and model distinct linear regimes in bead motion, we developed a multi-line fitting procedure using change-point theory. Briefly, regions of enzymatic activity are modeled by recursively fitting line pairs to smaller and smaller subregions. During each fitting cycle the most likely time point where a change in rate occurred is used as the location where one line ends and the next begins. The line pair resulting from this procedure defines the next two subregions for analysis. To avoid over fitting, only two-line fits above a threshold value are accepted (corresponding to a 1% false positive rate given the experimental error). This procedure allows for automated analysis of the experimental observations resulting in a complete list of distinct regions and their corresponding kinetics (**Figure 3C**).

Priming and lagging-strand synthesis underlie looping

Two types of DNA loops with distinct kinetics have been hypothesized to form during replication: ss and ss-ds loops. While ss loops grow at the rate of leading-strand synthesis, ss-ds loops grow as the sum of both polymerase synthesis rates (**Figure 1**). To classify the observed DNA loops, we constructed a two-dimensional map of loop growth vs. leading-strand synthesis using the results of kinetic change-point analysis from 53 individual molecules (**Figure 4A**). The map shows the location and relative weight (indicated with a color scale) of all individual pairs of leading and lagging-strand synthesis rates, providing a global view of the frequency of visits to different kinetic states by replisomes. Analysis of the loop-growth rates reveals two broad populations described well by two Gaussians (105 ± 28 bp·s^{-1}, 234 ± 54 bp·s^{-1}), consistent with the formation of both loop types. In contrast, leading-strand synthesis is best fit by a single Gaussian (128 ± 55 bp·s^{-1}). Based on the observed kinetics, we classify the slow loop-growth events as ss loops, having approximately the same rate as leading-strand synthesis, and the fast events as ss-ds loops, showing nearly twice the rate of synthesis.

Several additional and independent lines of evidence support the idea that the observed DNA shortening in the parental strand (bead *A*) is the result of both ss- and ss-ds-loop formation. Exploiting the high efficiency of single bead labeling of DNA molecules, we explored experimental conditions that alter looping dynamics with only parental-strand beads (A) present. First, we inhibited priming by omitting rNTPs and observed that looping was abolished (**Figure 4B**), consistent with inhibition of both priming and lagging-strand synthesis. Second, we conducted experiments by pre-loading the leading-strand polymerase and gp4 helicase–primase onto the DNA, and starting replication only in the presence of gp2.5, dNTPs, and rNTPs. These conditions selectively prevent ss-ds loop formation due to the absence of lagging-strand polymerases (Lee et al., 2006; Loparo et al., 2011). Consistent with our initial classification, the faster loops were abolished, while the slower loops remained (**Figure 4C & S7**). Furthermore, the lengths of ss loops increased when only the leading-strand polymerase was present (**Figure 4D** cf. **Figure 4E**), which is expected due to the absence of lagging-strand polymerases available for primer hand-off.

Examination of loop-formation frequencies reveals that ss loops form five times more often than ss-ds loops (**Figure 4F**). Moreover, on average only 1% of the synthesis required to complete duplication of the lagging strand was observed among the 53 molecules

analyzed with simultaneous imaging. In contrast, we previously demonstrated in single-molecule experiments visualizing the replication of fluorescently stained DNA that the lagging strand is completely duplicated under our experimental conditions (Geertsema et al., 2014; Hamdan et al., 2009). We considered several explanations for these divergent observations. We first excluded the possibility that the applied force inhibits loop formation by confirming similar looping dynamics at lower stretching forces (**Figure 4G, 4H, & S8**). We next evaluated alternative coordination mechanisms given recent observations of rapid polymerase exchange (Geertsema et al., 2014; Loparo et al., 2011) and the presence of more than two polymerases at the replication fork (Geertsema et al., 2014; McInerney et al., 2007; Reyes-Lamothe et al., 2010). Taken together, our results and these previously reported findings suggest a scenario in which most lagging-strand synthesis is conducted behind the replisome and outside the context of ss-ds loops.

Lagging-strand polymerases remain behind the replisome

Recent work examining the composition of the replisome during replication has revealed that polymerase exchange is a frequent event (Geertsema et al., 2014; Loparo et al., 2011), occurring on the same timescale as Okazaki-fragment synthesis. These observations cast doubt on the classic model of replication in which polymerases are retained within the replisome and recycled from one Okazaki fragment to the next. The triggers for the recycling process are proposed to be either a signaling event (by a protein factor or catalytic step) or a collision event (when the lagging-strand polymerase reaches the previous Okazaki fragment). However, if a new polymerase is used for the synthesis of almost every Okazaki fragment, as suggested by previous exchange observations (Geertsema et al., 2014), these pathways are not required. Supporting this line of reasoning, several studies have suggested that no specific protein factor exists for signaling (Kurth et al., 2013), and that collision events are orders of magnitude too slow to support efficient replication (Dohrmann et al., 2011). These findings suggest polymerase release is a stochastic event with many possible triggers. The previously reported single-molecule observations of polymerase exchange (Geertsema et al., 2014; Loparo et al., 2011) present the possibility that polymerases may remain bound to Okazaki fragments outside the context of a loop behind the replisome and that a new polymerase is recruited from solution to initiate synthesis of the next Okazaki fragment.

To visualize how individual DNA polymerases are spatially and temporally distributed in and around the replisome we conducted rolling-circle replication with fluorescently labeled

polymerases and imaged the products using fluorescence time-lapse microscopy (**Figure 5A**). The rolling-circle template allows for continuous synthesis of a single product with the replisome clearly visible at the tip and the lagging-strand extending behind, thereby greatly simplifying polymerase tracking and analysis. Processive replication events reveal polymerases remaining on the lagging strand behind the replisome (**Figure 5B**). Some polymerases remain bound on the lagging strand for very long times (minutes) consistent with stalling upon completion of Okazaki-fragment synthesis (Dohrmann et al., 2011; Huber et al., 1987). Examination of kymographs from 55 replication events reveals that polymerase emergence from the replication fork is four times more frequent than direct binding from solution to the lagging-strand (**Figure 5C & S10**), and the mean spacing between polymerases is 3.8 ± 0.4 kb, consistent with most polymerases rapidly completing Okazaki-fragment synthesis near the replication fork and dissociating (**Figure 5D**). The average number of polymerases per replisome spot is 2.6 ± 0.8, in good agreement with past observations from Geertsema et al. (2014). The average number of polymerases per spot on the lagging-strand is 1.5 ± 0.5, consistent with single polymerases left behind given the exponential distribution of polymerase spacing combined with the diffraction limit resulting in two or three polymerases in some spots (**Figure S11**). Further, we showed that the presence of T7 exonuclease and DNA ligase, the enzymes responsible for Okazaki-fragment processing, did not alter the distribution of polymerases on the lagging strand (**Figure S12**). Taken together, these observations are consistent with most lagging-strand synthesis being conducted outside the replisome, providing an explanation for the observed low number of ss-ds loops.

Priming is regulated by looping and pausing

Two mechanisms have been proposed that explain how the T7 replisome deals with slow primase activity (**Figure 1**). In one, priming pauses leading-strand synthesis (Lee et al., 2006). In the other, ss-loop formation permits leading-strand synthesis to continue during priming (Pandey et al., 2009). The observation of frequent ss-loop formation events, dependent on rNTPs and thus priming, strongly favors a coordination mechanism in which leading-strand synthesis continues during priming (Pandey et al., 2009). Nonetheless, detailed analysis of the leading-strand synthesis kinetics also reveals the existence of pausing events (**Figure 6A**). Pauses occur in approximately half of the molecules with a pause lifetime of 5.0 ± 0.7 s obtained from leading-strand bead (B) only observations (**Figure 6B**), consistent with previous estimates (Lee et al., 2006).

To understand the importance of pausing for coordination, we used the two-dimensional information contained within our observations and directly correlated the relative locations of pausing and looping events (**Figure 6C & D**). To quantify this relationship, we constructed a histogram of all pause positions relative to loop growth by normalizing the loop durations. This analysis shows that the vast majority of pausing events occur at the end of loop growth or right after loop release (**Figure 6D** & **S13**). Since almost all loops are ss loops, the results of this analysis are consistent with past observations of pause frequency increasing in conditions with priming (Lee et al., 2006). These findings further refine our understanding of pausing behavior extending it to show that, under conditions of coordinated replication, pauses only occur during or after completion of some priming events. Pauses are half as frequent as ss loops and not all pauses occur during loop release (**Figure 6D**).

Discussion

A Unified Model for Primer Synthesis Regulation

Our results reconcile divergent priming models and provide new insights into past observations. In a prior study, we reported single-molecule observations of loop formation (Hamdan et al., 2009) using a flow-stretching assay with only a single bead attached to the parental strand. Observations with this single observable lead to the conclusion that all loops during coordinated T7 replication are ss-ds loops. The independent readout of leading-strand synthesis from the two-bead assay presented here, provides critical information previously absent, revealing that the looping behavior observed represents a mixture of both ss and ss-ds loop types, instead of exclusively ss-ds loops as previously suggested (Hamdan et al., 2009).

A long-standing question in the field of replication has been whether the behavior of subsystems of the replisome are different than their activity in the context of the unified whole. The models for priming discussed in this work support two divergent views. In one, priming sets the clock for the replication fork by transiently stalling synthesis, in the other, the leading strand is less influenced by the events on the lagging strand. The ability to correlate events on the leading and lagging strands has allowed us to evaluate these ideas directly. The observation that pauses tend to punctuate looping events, provides a more detailed view of enzymatic coordination within the replisome. Why only some priming events lead to pausing, and whether these pauses are involved in synchronization or are simply a byproduct of the complex acrobatics required to orchestrate the process (Corn et

al., 2005; Lee and Richardson, 2002), will require further studies beyond the scope of this work. However, the observed correspondence between pausing and looping reveals how communication among replisome subsystems may enhance coordination, and demonstrates an underlying flexibility in the regulation of primer synthesis.

Multiple pathways underlie replisome coordination

Our findings suggest a timeline for the sequence of events that occur during phage T7 replication (**Figure 7**). The process begins with unwinding of parental duplex DNA by the helicase coupled to synthesis by the leading-strand polymerase (**Figure 7; panel A**). As the leading-strand complex progresses, the primase subunits within gp4 continuously sample the lagging-strand template as it emerges from the helicase. Once a priming site sequence is recognized and engaged, priming proceeds in two steps. First, two rNTPs are condensed into a dinucleotide, followed by extension into a full tetranucleotide primer (Frick et al., 1999; Swart and Griep, 1995). Leading-strand synthesis is continuous during this process resulting in ss loop formation (**Figure 7; panel B**). Upon completion of primer synthesis, a polymerase bound to the helicase loads onto the primer (**Figure 7; panel C**). Infrequently, stalling of leading-strand synthesis occurs, consistent with our previously observed primase-induced halting of leading-strand synthesis (Lee et al., 2006). Our proposed pathway diverges most significantly from past work in the next stage: Our data show the majority of polymerase loading events on the lagging strand culminate in polymerase release from the helicase (**Figure 7; panel E**), consistent with recently observed high frequencies of polymerase exchange at the fork (Geertsema et al., 2014). Okazaki-fragment synthesis would then proceed behind the replisome, with ss-ds looping events (**Figure 7; panel D**) only happening in rare cases where polymerase exchange is slow.

Several features of our proposed sequence of events confer robustness to replisome operation. First, ss loop formation removes the need for a direct signal to stop leading-strand synthesis during each cycle of lagging-strand synthesis, dramatically simplifying the communication required within the replisome (Manosas et al., 2009; Pandey et al., 2009). Second, the frequent release of polymerases from the helicase upon completion of loading rapidly frees up additional polymerase binding sites on the helicase allowing more polymerases to associate with the replisome and become available for loading onto new primers. Third, by forgoing polymerase recycling and allowing for completion of Okazaki-fragment synthesis after polymerase release, the T7 replication machinery has more time

to conduct primer synthesis and polymerase loading at the fork. Such a mechanism aids in ensuring that leading-strand synthesis does not outpace lagging-strand synthesis. Furthermore, polymerase dissociation from the lagging strand during Okazaki-fragment synthesis does not require signaling or collision mechanisms of regulation. Overall, these characteristics support the idea that T7 replisomes have a narrower operational mandate than previously thought whereby polymerases must be efficiently targeted to primers, but can then readily exchange to reset the cycle.

Implications for Replication Coordination

Conservation of replisome architecture throughout the domains of life suggests replication may be guided by the same operating principles in different systems, but defining that set of operating principles for even one system has proven challenging. Many competing coordination mechanisms have been proposed based on observations made under a wide range of experimental conditions and, in many cases, using only a subset of replisome components. Our ability to simultaneously visualize leading-strand synthesis and loop formation represents a significant advance in studying coordination within fully reconstituted replisomes. The results from this work provide a holistic view of the replication cycle, revealing that many previously proposed mechanisms of coordination, which were considered incompatible, are all employed at some frequency.

Sampling of different coordination mechanisms by replisomes is guided in part by physical constraints. In the case of T7, we observe that priming on the lagging strand is most frequently coordinated with leading-strand synthesis through the formation of a ss loop, and only in rare cases by pausing of leading-strand synthesis. However, in T7, primase and helicase activities are conducted by a single protein that assembles into a hexameric ring (gp4). In contrast, replisomes from other organisms, such as *E. coli*, use separate proteins to conduct helicase and primase activities. This added complexity and separation of enzymatic function allows for a broader range of coordination pathways—priming activity could occur in the absence of ss looping or pausing (Dixon, 2009). Primases may be released from the replisome to complete priming behind the fork (Yuzhakov et al., 1999). This complexity increases further in eukaryotic systems, with the use of different polymerases for leading- and lagging-strand synthesis as well as primer extension (Georgescu et al., 2014; Johansson and Dixon, 2013; Kunkel and Burgers, 2008).

In addition to physical restrictions, sampling of divergent coordination mechanisms is influenced by environmental factors. While exchange can be frequent under conditions with excess replication components in the surroundings, replisomes can also be stable in the absence of excess protein and continue replicating long after excess components have been removed from the reaction (Debyser et al., 1994; Kadyrov and Drake, 2001; Kim et al., 1996; Tanner et al., 2011; Yao et al., 2009). While these two observations may appear to contradict one another, it is likely that the presence of excess components in solution directly drives these exchange events by initiating a competition between binding sites at the replication fork (Geertsema et al., 2014; Geertsema and van Oijen, 2013; Tanner et al., 2011). In the case of the polymerases, these binding surfaces interfacing with the replisome are numerous including attachment points to the primer, the helicase or clamp loader, and even, in some cases, single-stranded binding proteins (Duderstadt et al., 2014; Hamdan and Richardson, 2009). In the absence of competition, polymerases can continually sample all these sites at the replication fork providing multiple points of contact, ensuring a stable attachment. However, under conditions of competition, the relatively low affinity of the individual interactions within the replisome allows polymerases from solution to quickly outcompete those at the fork, driving polymerase exchange and release (Aberg et al., 2016; Geertsema and van Oijen, 2013).

Based on our observations, we envision a spectrum of exchange frequencies and coordination mechanisms among replication systems. The bacteriophage T7 replisome may sit at one extreme of this spectrum, with polymerase exchange and the rapid release of ss-ds loops underling almost every cycle of Okazaki-fragment synthesis. Cellular replisomes, such as from *E. coli*, have proven more robust in the absence of free polymerase in solution (Yao et al., 2009) suggesting less frequent polymerases exchange. Nonetheless, the observation of multiple polymerases at the replication fork is consistent with multiple simultaneous rounds of lagging-strand synthesis ensuring coordination (Geertsema et al., 2014; Georgescu et al., 2012; Reyes-Lamothe et al., 2010). Recent work in *S. cerevisiae* has further expanded this picture by suggesting that rapid exchange and complex suppression mechanisms ensure proper function of the leading- and lagging-strand polymerases at the eukaryotic replication fork (Georgescu et al., 2014), supporting the notion that ss-ds loop formation may not be required for efficient replication in eukaryotes. The importance of exchange events and the sampling of multiple coordination pathways remains enigmatic in many cases, but clearly such processes are critical when considering that robust replication in cells depends on the ability of replisomes to

overcome obstacles encountered on parental chromosomes, such as transcription complexes and DNA lesions (Cox et al., 2000; Pomerantz and O'Donnell, 2010; Yeeles et al., 2013).

Experimental Procedures

Two-bead DNA Replication assay

Two-arm λ-phage DNA substrates were surface-tethered inside flowcells constructed by placing PDMS lids over functionalized coverslips. Inlets and outlets in the PDMS allowed for buffer exchange and introduction of MyOne Tosylactivated paramagnetic beads (1 μm diameter, Life technologies) functionalized with anti-fluorescein (Life technologies) and anti-digoxigenin (Roche). Beads were added together except where otherwise specified. Coordinated DNA synthesis reactions were initiated with purified gp4 helicase–primase (10 nM hexamers) , T7 DNA polymerase (a 1:1 complex of gp5 and thioredoxin, 80 nM), gp2.5 (4 μM) in buffer A (40 mM Tris–HCl (pH 7.5), 10 mM $MgCl_2$, 10 mM DTT, 50 mM potassium glutamate (pH 7.5), 0.1 mg/ml BSA) containing 600 μM dATP, 600 μM dCTP, 600 μM dGTP, 600 μM dTTP, 300 μM ATP and 300 μM CTP. The beads were illuminated from the side with a fiber illuminator (ThorLabs) and movies were collected using a 29 Megapixel CCD camera (Prosilica GX6600; Allied Vision Technologies; 5.5 μm pixel size) with Streampix imaging software (Norpix) at either magnification 4X (UPLSAPO; Olympus) on an IX51 microscope (Olympus) or magnification 7X with a lens (TL12K-70-15; lensation) mounted directly to the camera. Replication was monitored by tracking the motion of the beads and converting changes in position to basepairs using custom ImageJ plugins programmed in house. Kinetic change-point anaylsis yielded similar results for movies collected with 2 and 4 fps, so data presented were collected at 2 fps for computational convenience.

Kinetic change-point algorithm and distribution construction

To extract detailed kinetic information from complex two-bead observations we developed a novel multi-line fitting procedure inspired by an algorithm developed for modeling fluorescence intensity data (Yang, 2011). Bead motion was modeled by recursively fitting line pairs to smaller and smaller subregions. During each fitting cycle the most likely position for a change in motion (kinetic change-point) defined each segment, and each currently fit segment defined the boundaries for the next cycle of analysis. To avoid over fitting, pairs of line segments below a threshold value were rejected (corresponding to a 1% false positive rate given the error model). Tethered beads undergo Brownian fluctuations, which can be modeled using a Gaussian error model. For such an error model the likelihood of observing the set of positions $(X|Y)$ given experimental error σ for a line of slope a_k and intercept b_k is

$$L(Y|X; a_k, b_k) = \prod_{i=1}^{N} \frac{1}{\sqrt{2\pi\sigma^2}} e^{-\frac{(y_i - a_k * x_i - b_k)^2}{2\sigma^2}}.$$

To evaluate the relative likelihood of a two line fits versus a single line fit, within a given region, we searched for the most likely positions of kinetic change-points using the likelihood ratio:

$$L_N(k) = \frac{L_N(\text{two lines})}{L_N(\text{one line})} = \frac{L_A * L_B}{L_0}.$$

The maximum value of this ratio was taken as the most likely position for a kinetic change-point. In practice, working with the log of this ratio provided additional computational convenience. Moreover, the threshold value of this log-likelihood ratio corresponding to a 1% false positive rate is easily calculated numerically using a closed-form expression (Yang, 2011).

Once all kinetic change-points above the threshold were determined, rate distributions were constructed using the slopes from single line fits between each set of consecutive kinetic changepoints. To properly account for experimental uncertainty, each slope estimate and associated standard error were used to define a Gaussian. These Gaussians were time-weighted, summed and binned to generate the final distributions seen in **Figures 4A, 4B, 4C**. The loop length and type histograms seen in **Figures 4D** and **4E** were generated using ss and ss-ds looping events as defined by segment slopes below and above a cutoff of 175 bp/s as indicated by a dashed line in **Figures 4A**. For the low force condition of 0.7 pN, the length of gp2.5-coated ssDNA remains 73% that of dsDNA, so the same cutoff of 175 bp/s was used in generating **Figures 4F, 4G**, and **4H**. The pause duration histogram seen in **Figure 6B** was generated using the lifetimes of line segments exhibiting at least a 3-fold reduction in rate to a value below 50 bp s^{-1}. Only twenty pauses were observed in the two-bead dataset, which was not sufficient for a reliable estimate of the mean duration of pauses. Therefore, leading-strand bead (B) observations made with the same conditions were used to determine the mean pause duration (**Figure 6B**). In all cases, consecutive lines within the same slope range were considered as single events, and their lifetimes were added. All error bars represent the standard deviation (SD) from 100 cycles of randomly resampling the data by bootstrapping. The uncertainties reported for the exponential fits in **Figures 4D, 4E, 4H, 5D, 6B** represent the standard deviation of the mean values from fits of all resampled distributions.

Fluorescence time-lapse microscopy of labeled polymerases

T7 DNA polymerases labelled with Alexa Fluor 488 and M13 rolling-circle replication substrates were generated as previously described (Geertsema et al., 2014). Coordinated replication was established using a constant flow of purified gp4 helicase–primase (2.5 nM hexamers), Alexa488-labeled T7 DNA polymerase (a 1:1 complex of gp5 and thioredoxin, 20 nM), gp2.5 (1 μM) in buffer A containing 600 μM dATP, 600 μM dCTP, 600 μM dGTP, 600 μM dTTP, 300 μM ATP and 300 μM CTP. The proteins were diluted 4-fold as compared to the bead experiments, which was necessary for imaging of single polymerases. Labeled polymerases were illuminated with a 488-nm laser (Coherent) through a 60× TIRF objective [Olympus, UApoN, N.A. = 1.49 (oil)] and image sequences were captured with an EMCCD camera (Andor) using Micro-Manager imaging software at 5 fps. A detailed description of the image processing procedure can be found in the Supplemental Experimental Procedures.

Code availability

All analysis was performed using custom ImageJ plugins programmed in house. Source code for most analysis tools is available at GitHub under Single Molecule Biophysics plugins for ImageJ. Source code used for kinetic change-point analysis is provided upon request.

Supplemental Data

Supplemental Data includes Supplemental Experimental Procedures, eleven figures, one table and three movies.

Author Contributions

K.E.D. designed, conducted, and analyzed the single-molecule bead experiments. H.J.G. and K.E.D conducted, and analyzed the single-molecule fluorescence experiments. S.A.S., A.W.K., and C.C.R. prepared proteins. C.M.P. and K.E.D wrote software used for analysis of the single-molecule data. K.E.D. and A.v.O. directed the project and wrote the paper with input from all authors.

Acknowledgments

We thank Nick Dixon, Jack Griffith, and members of the van Oijen lab for helpful discussions and critical feedback. We also thank Victor Krasnikov for instrumentation support. This work was funded by an ERC Starting grant (281098; SINGLEREPLISOME),

an NWO Vici grant (680-47-607), and an Australian Research Council Laureate Fellowship (FL140100027) to AvO, as well as a Human Frontier Science Program Fellowship and support from the Max Planck Society to KED.

References

Aberg, C., Duderstadt, K.E., and van Oijen, A.M. (2016). Stability versus exchange: a paradox in DNA replication. Nucleic Acids Res *44*, 4846-4854.

Alberts, B.M., Barry, J., Bedinger, P., Formosa, T., Jongeneel, C.V., and Kreuzer, K.N. (1983). Studies on DNA replication in the bacteriophage T4 in vitro system. Cold Spring Harbor symposia on quantitative biology *47 Pt 2*, 655-668.

Chastain, P.D., 2nd, Makhov, A.M., Nossal, N.G., and Griffith, J. (2003). Architecture of the replication complex and DNA loops at the fork generated by the bacteriophage t4 proteins. The Journal of biological chemistry *278*, 21276-21285.

Corn, J.E., Pease, P.J., Hura, G.L., and Berger, J.M. (2005). Crosstalk between primase subunits can act to regulate primer synthesis in trans. Mol Cell *20*, 391-401.

Cox, M.M., Goodman, M.F., Kreuzer, K.N., Sherratt, D.J., Sandler, S.J., and Marians, K.J. (2000). The importance of repairing stalled replication forks. Nature *404*, 37-41.

Debyser, Z., Tabor, S., and Richardson, C.C. (1994). Coordination of leading and lagging strand DNA synthesis at the replication fork of bacteriophage T7. Cell *77*, 157-166.

Dixon, N.E. (2009). DNA replication: prime-time looping. Nature *462*, 854-855.

Dohrmann, P.R., Manhart, C.M., Downey, C.D., and McHenry, C.S. (2011). The rate of polymerase release upon filling the gap between Okazaki fragments is inadequate to support cycling during lagging strand synthesis. J Mol Biol *414*, 15-27.

Duderstadt, K.E., Reyes-Lamothe, R., van Oijen, A.M., and Sherratt, D.J. (2014). Replication-fork dynamics. Cold Spring Harbor perspectives in biology *6*.

Frick, D.N., Kumar, S., and Richardson, C.C. (1999). Interaction of ribonucleoside triphosphates with the gene 4 primase of bacteriophage T7. J Biol Chem *274*, 35899-35907.

Geertsema, H.J., Kulczyk, A.W., Richardson, C.C., and van Oijen, A.M. (2014). Single-molecule studies of polymerase dynamics and stoichiometry at the bacteriophage T7 replication machinery. Proc Natl Acad Sci U S A.

Geertsema, H.J., and van Oijen, A.M. (2013). A single-molecule view of DNA replication: the dynamic nature of multi-protein complexes revealed. Curr Opin Struct Biol *23*, 788-793.

Georgescu, R.E., Kurth, I., and O'Donnell, M.E. (2012). Single-molecule studies reveal the function of a third polymerase in the replisome. Nat Struct Mol Biol *19*, 113-116.

Georgescu, R.E., Langston, L., Yao, N.Y., Yurieva, O., Zhang, D., Finkelstein, J., Agarwal, T., and O'Donnell, M.E. (2014). Mechanism of asymmetric polymerase assembly at the eukaryotic replication fork. Nat Struct Mol Biol.

Hamdan, S.M., Loparo, J.J., Takahashi, M., Richardson, C.C., and van Oijen, A.M. (2009). Dynamics of DNA replication loops reveal temporal control of lagging-strand synthesis. Nature *457*, 336-339.

Hamdan, S.M., and Richardson, C.C. (2009). Motors, switches, and contacts in the replisome. Annu Rev Biochem *78*, 205-243.

Huber, H.E., Tabor, S., and Richardson, C.C. (1987). Escherichia coli thioredoxin stabilizes complexes of bacteriophage T7 DNA polymerase and primed templates. J Biol Chem *262*, 16224-16232.

Johansson, E., and Dixon, N. (2013). Replicative DNA polymerases. Cold Spring Harbor perspectives in biology *5*.

Kadyrov, F.A., and Drake, J.W. (2001). Conditional coupling of leading-strand and lagging-strand DNA synthesis at bacteriophage T4 replication forks. J Biol Chem *276*, 29559-29566.

Kim, S., Dallmann, H.G., McHenry, C.S., and Marians, K.J. (1996). tau couples the leading- and lagging-strand polymerases at the Escherichia coli DNA replication fork. J Biol Chem *271*, 21406-21412.

Kornberg, A., and Baker, T. (1992). DNA replication, 2nd edn (New York: Freeman).

Kunkel, T.A., and Burgers, P.M. (2008). Dividing the workload at a eukaryotic replication fork. Trends in cell biology *18*, 521-527.

Kurth, I., Georgescu, R.E., and O'Donnell, M.E. (2013). A solution to release twisted DNA during chromosome replication by coupled DNA polymerases. Nature *496*, 119-122.

Lee, J., Chastain, P.D., 2nd, Griffith, J.D., and Richardson, C.C. (2002). Lagging strand synthesis in coordinated DNA synthesis by bacteriophage t7 replication proteins. J Mol Biol *316*, 19-34.

Lee, J.B., Hite, R.K., Hamdan, S.M., Xie, X.S., Richardson, C.C., and van Oijen, A.M. (2006). DNA primase acts as a molecular brake in DNA replication. Nature *439*, 621-624.

Lee, S.J., and Richardson, C.C. (2002). Interaction of adjacent primase domains within the hexameric gene 4 helicase-primase of bacteriophage T7. Proc Natl Acad Sci U S A *99*, 12703-12708.

Li, X., and Marians, K.J. (2000). Two distinct triggers for cycling of the lagging strand polymerase at the replication fork. The Journal of biological chemistry *275*, 34757-34765.

Loparo, J.J., Kulczyk, A.W., Richardson, C.C., and van Oijen, A.M. (2011). Simultaneous single-molecule measurements of phage T7 replisome composition and function reveal the mechanism of polymerase exchange. Proceedings of the National Academy of Sciences of the United States of America *108*, 3584-3589.

Manosas, M., Spiering, M.M., Zhuang, Z., Benkovic, S.J., and Croquette, V. (2009). Coupling DNA unwinding activity with primer synthesis in the bacteriophage T4 primosome. Nat Chem Biol *5*, 904-912.

McInerney, P., Johnson, A., Katz, F., and O'Donnell, M. (2007). Characterization of a triple DNA polymerase replisome. Molecular cell *27*, 527-538.

Nelson, S.W., Kumar, R., and Benkovic, S.J. (2008). RNA primer handoff in bacteriophage T4 DNA replication: the role of single-stranded DNA-binding protein and polymerase accessory proteins. J Biol Chem *283*, 22838-22846.

Okazaki, R., Okazaki, T., Sakabe, K., Sugimoto, K., and Sugino, A. (1968). Mechanism of DNA chain growth. I. Possible discontinuity and unusual secondary structure of newly synthesized chains. Proc Natl Acad Sci U S A *59*, 598-605.

Pandey, M., Syed, S., Donmez, I., Patel, G., Ha, T., and Patel, S.S. (2009). Coordinating DNA replication by means of priming loop and differential synthesis rate. Nature *462*, 940-943.

Park, K., Debyser, Z., Tabor, S., Richardson, C.C., and Griffith, J.D. (1998). Formation of a DNA loop at the replication fork generated by bacteriophage T7 replication proteins. J Biol Chem *273*, 5260-5270.

Pomerantz, R.T., and O'Donnell, M. (2010). What happens when replication and transcription complexes collide? Cell Cycle *9*, 2537-2543.

Reyes-Lamothe, R., Sherratt, D.J., and Leake, M.C. (2010). Stoichiometry and architecture of active DNA replication machinery in Escherichia coli. Science (New York, N.Y.) *328*, 498-501.

Scherzinger, E., Lanka, E., and Hillenbrand, G. (1977). Role of bacteriophage T7 DNA primase in the initiation of DNA strand synthesis. Nucleic Acids Res *4*, 4151-4163.

Swart, J.R., and Griep, M.A. (1995). Primer synthesis kinetics by Escherichia coli primase on single-stranded DNA templates. Biochemistry *34*, 16097-16106.

Syed, S., Pandey, M., Patel, S.S., and Ha, T. (2014). Single-molecule fluorescence reveals the unwinding stepping mechanism of replicative helicase. Cell reports *6*, 1037-1045.

Tanner, N.A., Hamdan, S.M., Jergic, S., Loscha, K.V., Schaeffer, P.M., Dixon, N.E., and van Oijen, A.M. (2008). Single-molecule studies of fork dynamics in Escherichia coli DNA replication. Nature structural & molecular biology *15*, 998.

Tanner, N.A., Loparo, J.J., Hamdan, S.M., Jergic, S., Dixon, N.E., and van Oijen, A.M. (2009). Real-time single-molecule observation of rolling-circle DNA replication. Nucleic acids research *37*, e27.

Tanner, N.A., Tolun, G., Loparo, J.J., Jergic, S., Griffith, J.D., Dixon, N.E., and van Oijen, A.M. (2011). E. coli DNA replication in the absence of free beta clamps. The EMBO journal *30*, 1830-1840.

Yang, H. (2011). Change-Point Localization and Wavelet Spectral Analysis of Single-Molecule Time Series (Hoboken, NJ, USA: John Wiley & Sons, Inc.).

Yao, N.Y., Georgescu, R.E., Finkelstein, J., and O'Donnell, M.E. (2009). Single-molecule analysis reveals that the lagging strand increases replisome processivity but slows replication fork progression. Proceedings of the National Academy of Sciences of the United States of America *106*, 13236-13241.

Yeeles, J.T., Poli, J., Marians, K.J., and Pasero, P. (2013). Rescuing stalled or damaged replication forks. Cold Spring Harbor perspectives in biology *5*, a012815.

Yuzhakov, A., Kelman, Z., and O'Donnell, M. (1999). Trading places on DNA--a three-point switch underlies primer handoff from primase to the replicative DNA polymerase. Cell *96*, 153-163.

Figure Legends

Figure 1. Coordination Models. (A) Priming pauses the replisome to ensure that leading-strand synthesis does not outpace lagging-strand synthesis. (B) Helicase unwinding and leading-strand synthesis continue during priming by the formation of a lagging-strand ss loop emerging from the helicase. This configuration keeps the primer in close physical proximity to the fork facilitating hand-off to a lagging-strand polymerase. (C) Coupled leading- and lagging-strand synthesis leads to the formation of an ss-ds loop that grows as the sum of the ssDNA output of helicase activity and the synthesis rate of the lagging-strand polymerase. A detailed description of how the models were constructed can be found in the Supplement.

Figure 2. Experimental Setup. (A) Ultra-low-magnification single-molecule imaging. Tens of thousands of single molecules are imaged simultaneously with wide-field optical microscopy using a low-magnification, high-numerical-aperture objective. Top right: Representative image showing 27,000 beads collected at 4X magnification. Bottom left: A replication fork introduced into the middle of lambda DNA with bead attachment sites at each end. Bottom right: zoomed-in section of wide-field image depicting pair of beads attached to a DNA substrate. (B) Two-bead assembly stretched by flow with a long leading-strand arm and short parental strand arm.

Figure 3. Simultaneous Imaging of DNA looping and Leading-Strand Synthesis. (A) Operational modes of the replisome discriminated by the two-bead replication assay. (B) Observation of simultaneous leading- and lagging-strand synthesis (**Video S3**). Top: motion of leading-strand bead *B* (green) and leading-strand synthesis *B*-*A* (black). Bottom: corresponding motion of parental-strand bead *A* showing looping dynamics during replication (black) with loop growth and release events indicated by red and gray bars, respectively. Conversion of observed bead displacements (right axis) to DNA length changes (left axis) depends on careful consideration of all forces and distinct DNA regions (**Figure S6**). Additional traces can be seen in **Figure S5.** (C) Results of kinetic change-point analysis for the molecule shown in B. Red lines indicate segments fitted based on detected change-point positions.

Figure 4. Looping dynamics. (A) Two-dimensional map of leading-strand synthesis and loop growth events (N_{mol} = 53 molecules). Individual peaks represent the relative rates at given times determined by kinetic change-point analysis with widths defined by the

standard error from linear fitting. A scatter plot of peak positions can be seen in **Figure S9**. One-dimensional distributions are displayed for each axis (gray bars – top and right) with indicated peak rates obtained from Gaussian fits. (B) Parental-strand bead A assay showing that omitting rNTPs abolishes looping. (C) Parental-strand bead A assay showing that preassembling leading-strand replisomes with no lagging-strand polymerases abolishes ss-ds loops, but ss loops remain. In panels B and C the gray bars represent the loop growth rates (parental-strand bead *A*) from simultaneous observations of coordinated replication at 2 pN (same data as displayed in panel A), while the red bars represent observations of replication with only parental-strand bead *A* attached. (D) Parental-strand bead A assay showing that ss loop lengths increase in the absence of lagging-strand polymerases as compared to (E) ss loop lengths for simultaneous observations using conditions of coordinated leading- and lagging-strand synthesis. The gray bar represents undersampled short loops excluded from fitting. (F) The relative frequency of ss and ss-ds loops under fully coordinated conditions evaluated using the two-bead dataset. (G) Parental-strand bead A assay showing that the relative frequency of ss to ss-ds loops does not change when the applied force is reduced by three-fold (from 2 to 0.7 pN). (H) Ss loop length likewise remains unchanged by a three-fold reduction in force. The gray bar represents undersampled short loops excluded from fitting. In all cases, error bars represent the standard deviation (SD) from 100 cycles of randomly resampling the data by bootstrapping.

Figure 5. Polymerases remain bound to the lagging strand. (A) (left) Rolling-circle replication assay with replisome components colored as in **Figure 2B** with the addition of yellow circles representing the fluorescent labels for imaging. Replication results in a lengthening of the lagging strand that is stretched by flow. This allows the remaining polymerases to be distinguished from the replisome. (right) Example kymograph showing the positions of polymerases (white) during replication. (B) Replisome (gray) and polymerase (black) positions from tracking the polymerases displayed in panel A. Light blue regions represent standard error from tracking. (C) Frequency of polymerases emerging from the replisome versus binding directly to the lagging strand. (D) Histogram of polymerase spacing on the lagging strand (red bars; N_{mol} = 222) fit with a single-exponential decay (black line). Spacings shorter than 3 kb were not included in the fitting (gray bar) due to undersampling resulting from DNA fluctuations and the diffraction limit.

Figure 6. Pauses in leading-strand synthesis. (A) Representative pausing event in leading-strand synthesis (black) from a simultaneous leading- and lagging-strand observation (parental-strand bead *A* trace not shown). Red lines indicate segments fitted based on detected change-point positions with the upper left inset providing a close-up view. (B) Histogram of pause durations calculated from a leading-strand bead B only dataset (red bars; N_{mol} = 395) fit with a single-exponential decay (black line). (C) Example trajectory showing the correspondence of pausing in leading-strand synthesis (top – black line) to loop growth and release (bottom – black line) on the lagging strand. Red lines indicate segments fitted based on detected change-point positions. (D) Distribution of pause locations (bottom) relative to loop locations (top) normalized by the loop duration. In all cases, error bars represent the standard deviation (SD) from 100 cycles of randomly resampling the data by bootstrapping.

Figure 7. Life cycle of a replisome. Multiple pathways confer robustness to replisome operation. (A) The replisome conducts leading-strand synthesis while searching for a priming site. (B) During priming an ss loop grows on the lagging strand while leading-strand synthesis continues. Infrequently, this process causes pausing of leading-strand synthesis. (C) Completion of primer synthesis triggers polymerase loading onto the new primer. (D) Infrequently ss-ds loops form as the replisome performs Okazaki-fragment synthesis. (E) More often polymerases are released onto the lagging strand so that Okazaki fragment synthesis can be completed behind the replisome while the next round of primer synthesis and polymerase loading take place.

Coordination Models

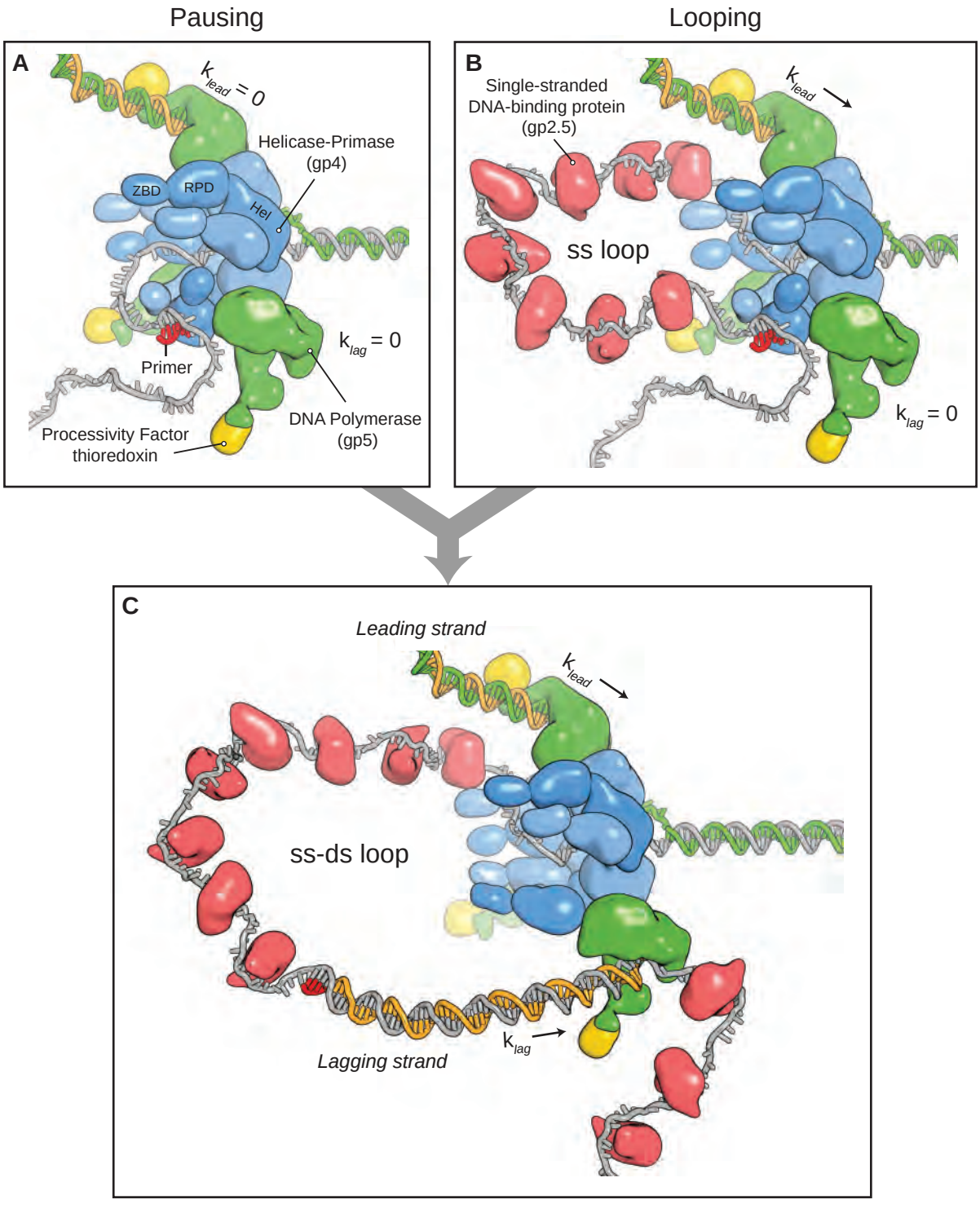

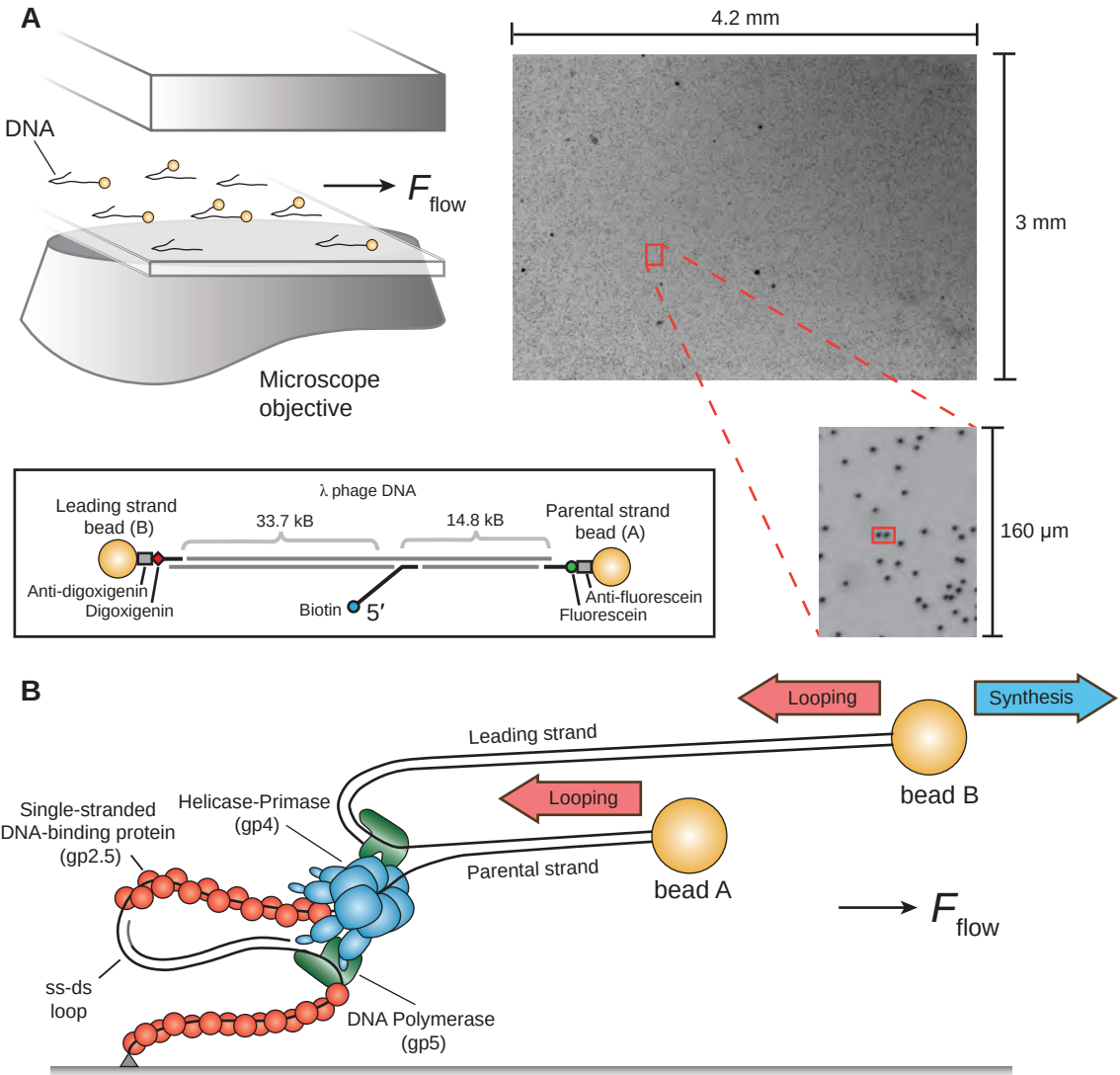
A
DNA
F flow
Microscope objective
4.2 mm
3 mm
160 μm
λ phage DNA
Leading strand bead (B)
33.7 kB
14.8 kB
Parental strand bead (A)
Anti-digoxigenin
Digoxigenin
Biotin
5′
Anti-fluorescein
Fluorescein
B
Looping
Synthesis
Leading strand
bead B
Looping
Single-stranded DNA-binding protein (gp2.5)
Helicase-Primase (gp4)
Parental strand
bead A
F flow
ss-ds loop
DNA Polymerase (gp5)

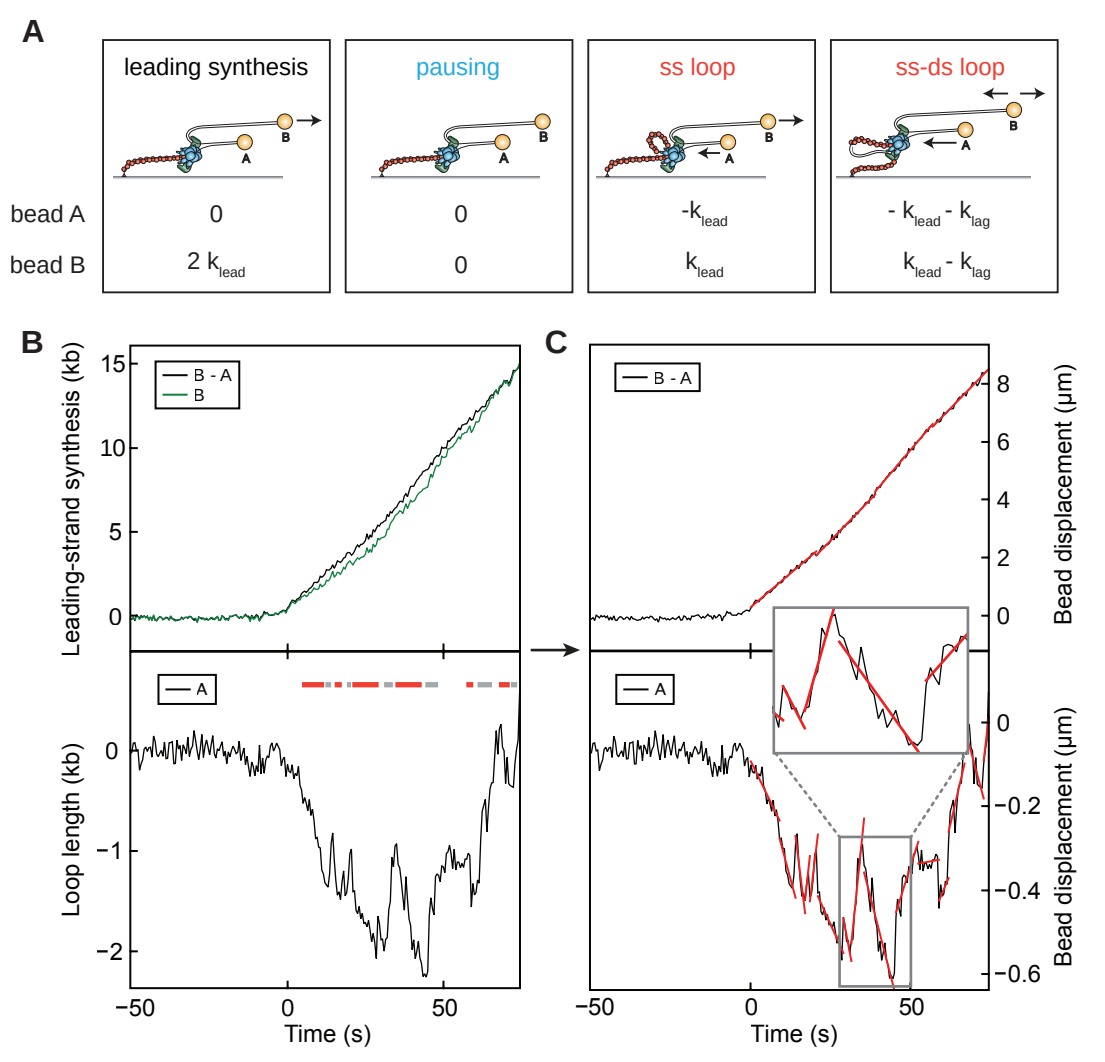
A
leading synthesis
pausing
ss loop
ss-ds loop
B
A
bead A
bead B
0
2 k lead
0
0
-k lead
k lead
- k lead - k lag
k lead - k lag
B
Leading-strand synthesis (kb)
B - A
B
A
Loop length (kb)
Time (s)
C
Bead displacement (µm)
Time (s)

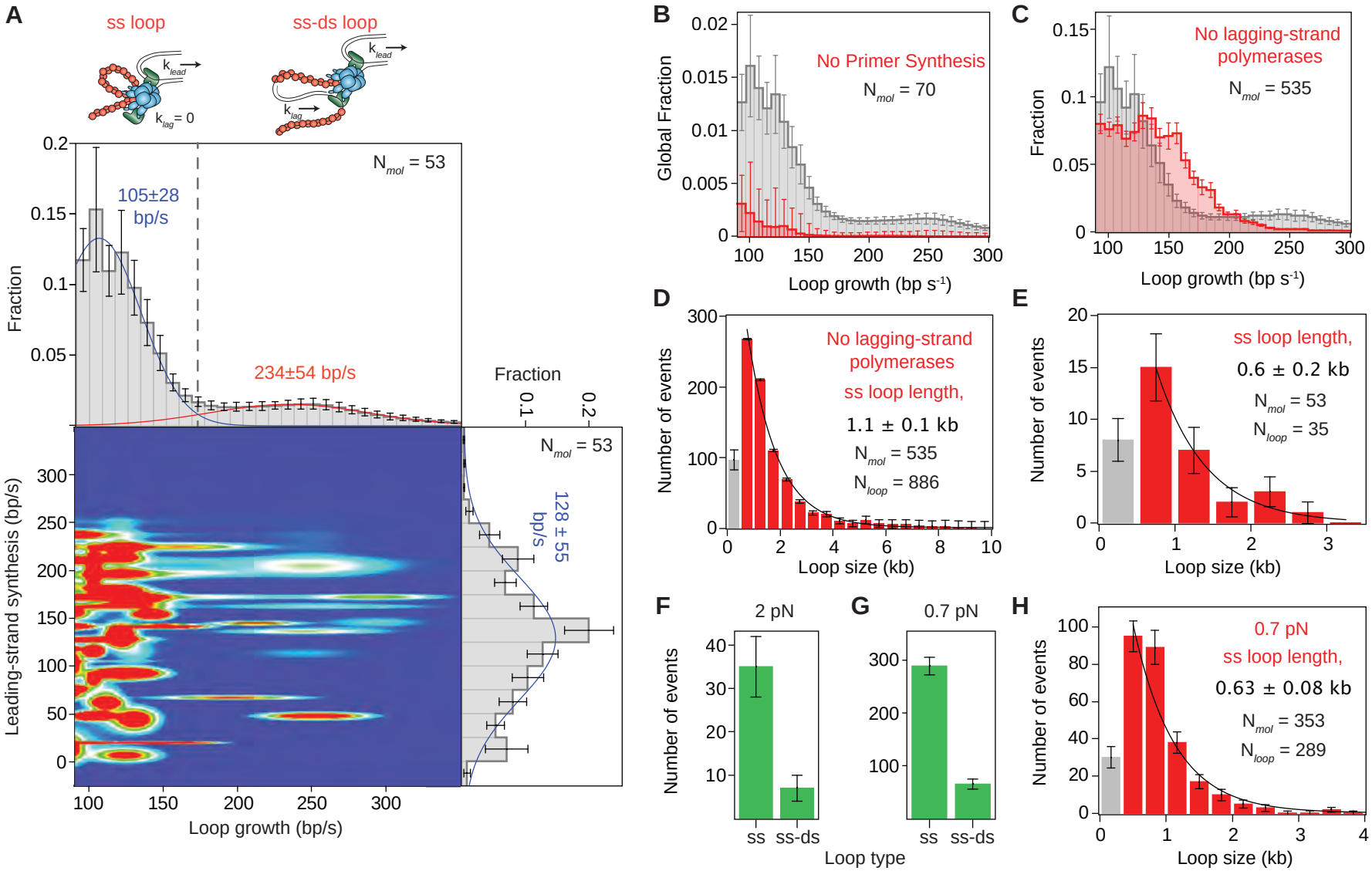
A
ss loop
ss-ds loop
k_lead
k_lag = 0
k_lag
N_mol = 53
105±28 bp/s
234±54 bp/s
Fraction
Leading-strand synthesis (bp/s)
Loop growth (bp/s)
128 ± 55 bp/s
B
No Primer Synthesis
N_mol = 70
Global Fraction
Loop growth (bp s-1)
C
No lagging-strand polymerases
N_mol = 535
Fraction
Loop growth (bp s-1)
D
No lagging-strand polymerases
ss loop length,
1.1 ± 0.1 kb
N_mol = 535
N_loop = 886
Number of events
Loop size (kb)
E
ss loop length,
0.6 ± 0.2 kb
N_mol = 53
N_loop = 35
Number of events
Loop size (kb)
F
2 pN
Number of events
ss
ss-ds
Loop type
G
0.7 pN
ss
ss-ds
H
0.7 pN
ss loop length,
0.63 ± 0.08 kb
N_mol = 353
N_loop = 289
Number of events
Loop size (kb)

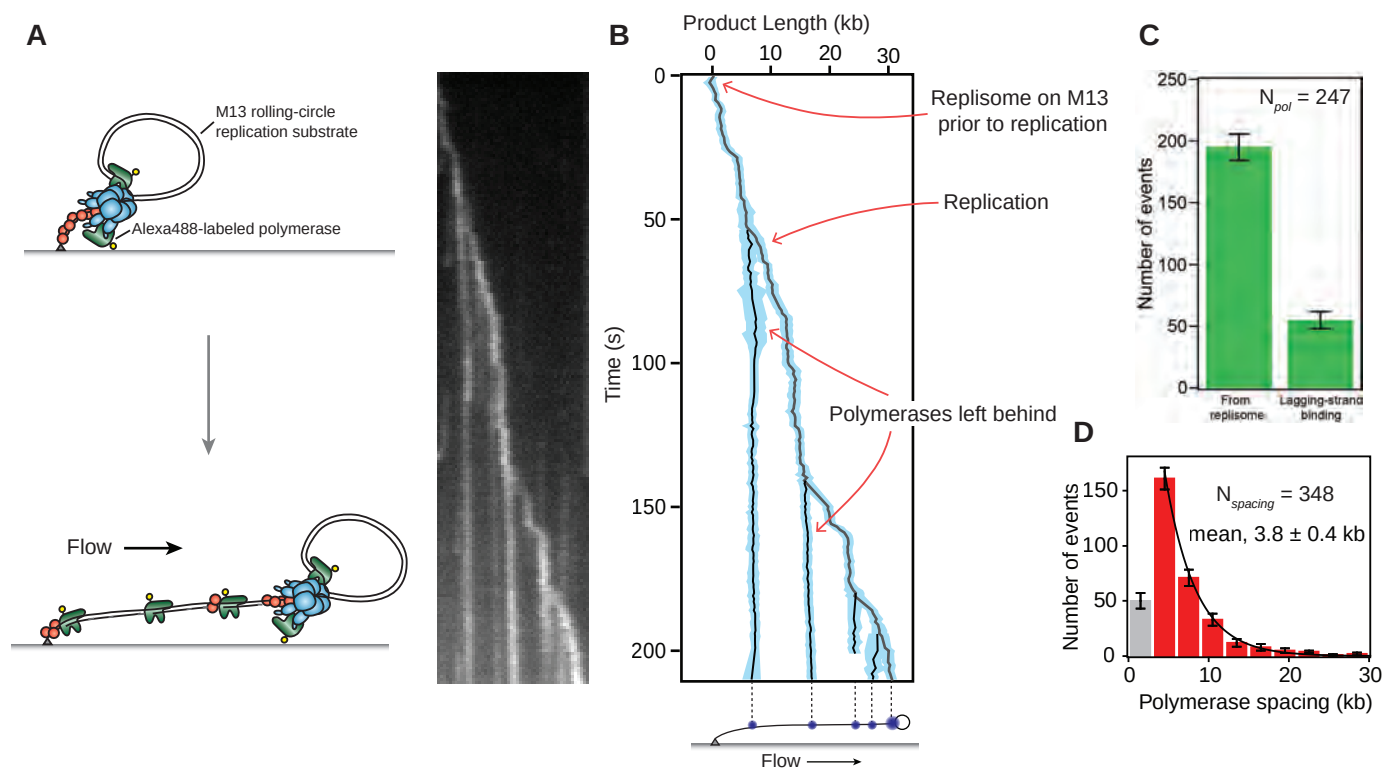
A
M13 rolling-circle replication substrate
Alexa488-labeled polymerase
Flow
B
Product Length (kb)
0
10
20
30
Time (s)
0
50
100
150
200
Replisome on M13 prior to replication
Replication
Polymerases left behind
Flow
C
N_{pol} = 247
Number of events
250
200
150
100
50
0
From replisome
Lagging-strand binding
D
$N_{spacing}$ = 348
mean, 3.8 ± 0.4 kb
Number of events
150
100
50
0
0
10
20
30
Polymerase spacing (kb)

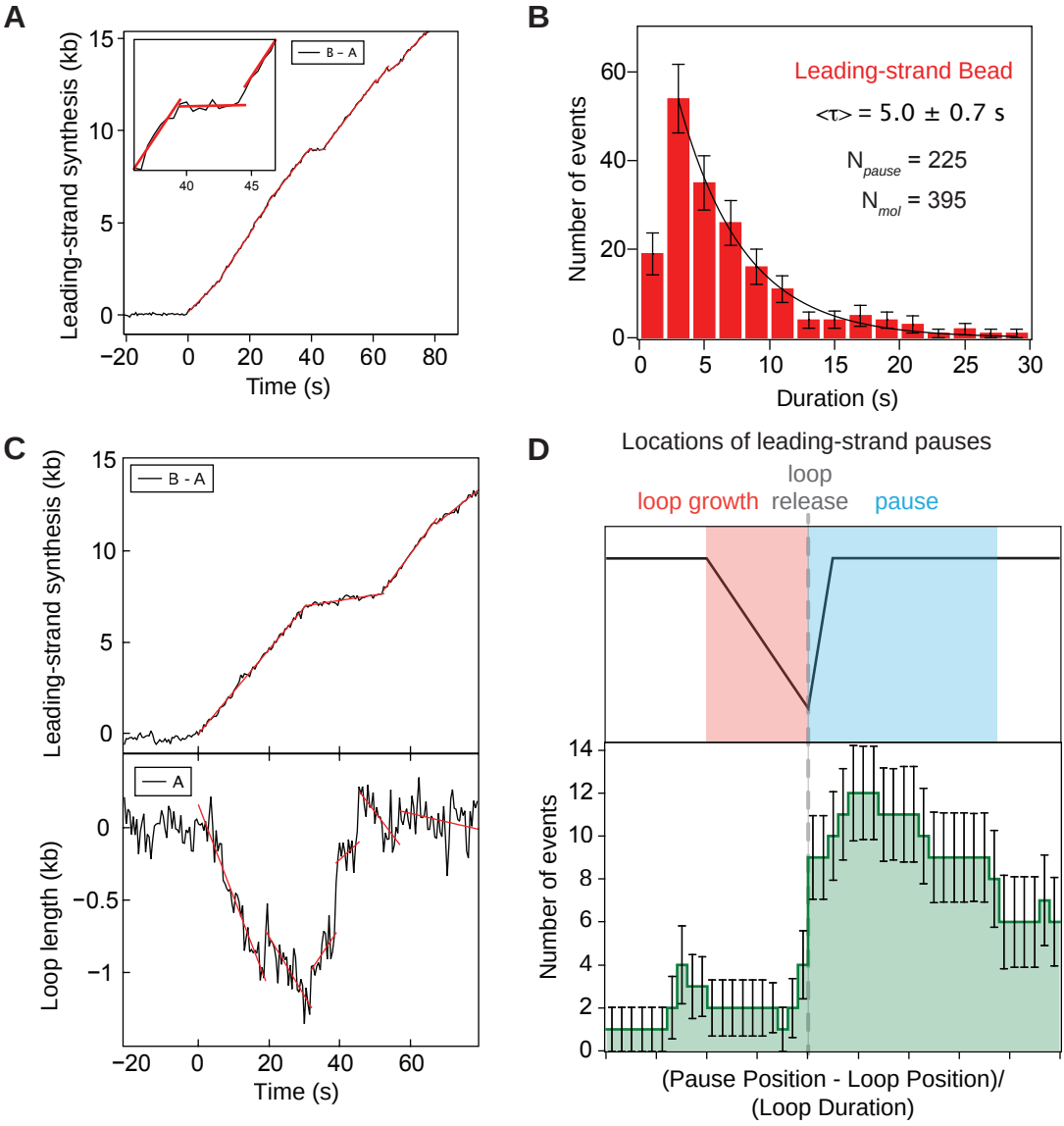
A
Leading-strand synthesis (kb)
B - A
Time (s)
B
Leading-strand Bead
<τ> = 5.0 ± 0.7 s
N_pause = 225
N_mol = 395
Number of events
Duration (s)
C
Leading-strand synthesis (kb)
B - A
A
Loop length (kb)
Time (s)
D
Locations of leading-strand pauses
loop growth
loop release
pause
Number of events
(Pause Position - Loop Position)/
(Loop Duration)

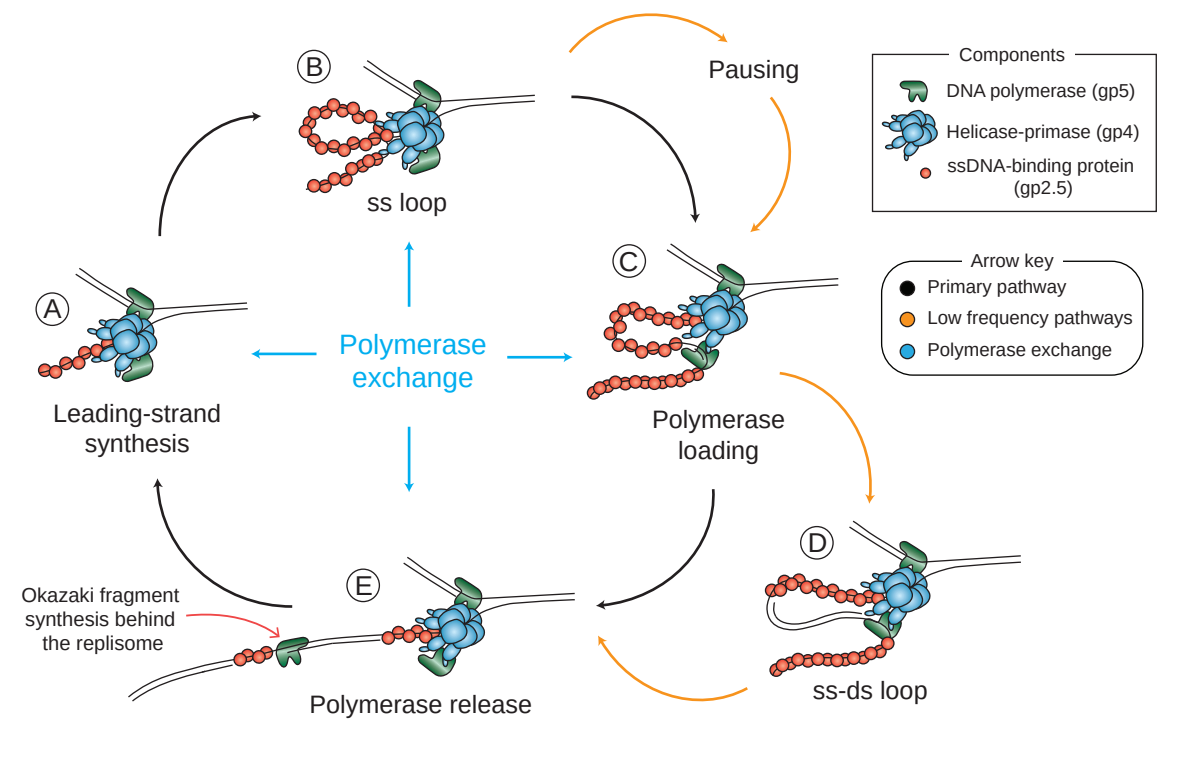
Components
DNA polymerase (gp5)
Helicase-primase (gp4)
ssDNA-binding protein (gp2.5)
Arrow key
Primary pathway
Low frequency pathways
Polymerase exchange
A
Leading-strand synthesis
B
ss loop
C
Polymerase loading
D
ss-ds loop
E
Polymerase release
Pausing
Polymerase exchange
Okazaki fragment synthesis behind the replisome

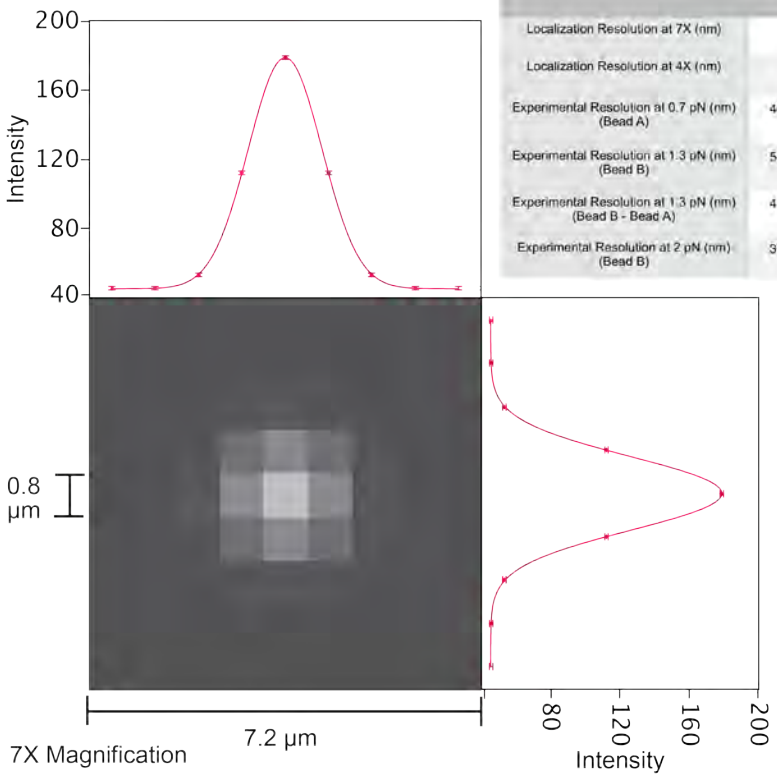

	σ_x	σ_y
Localization Resolution at 7X (nm)	5.0	5.0
Localization Resolution at 4X (nm)	8.7	8.7
Experimental Resolution at 0.7 pN (nm) (Bead A)	46 (170 bps)	-
Experimental Resolution at 1.3 pN (nm) (Bead B)	54 (180 bps)	-
Experimental Resolution at 1.3 pN (nm) (Bead B - Bead A)	41 (130 bps)	-
Experimental Resolution at 2 pN (nm) (Bead B)	37 (120 bps)	-

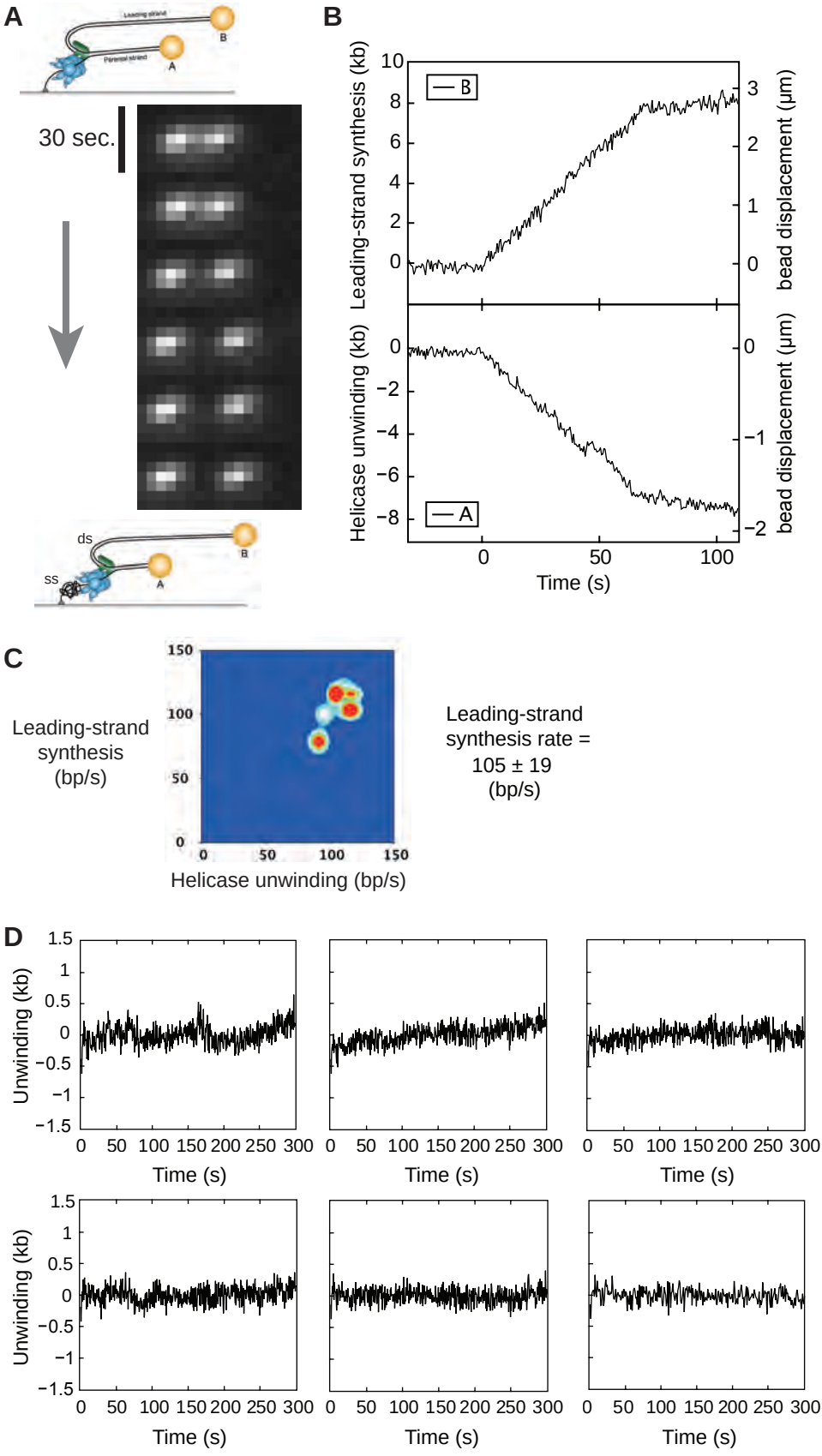
A
B
Leading strand
Parental strand
B
A
30 sec.
ds
ss
B
A
B
Leading-strand synthesis (kb)
bead displacement (μm)
Helicase unwinding (kb)
bead displacement (μm)
A
Time (s)
C
Leading-strand synthesis (bp/s)
Helicase unwinding (bp/s)
Leading-strand synthesis rate = 105 ± 19 (bp/s)
D
Unwinding (kb)
Time (s)
Unwinding (kb)
Time (s)

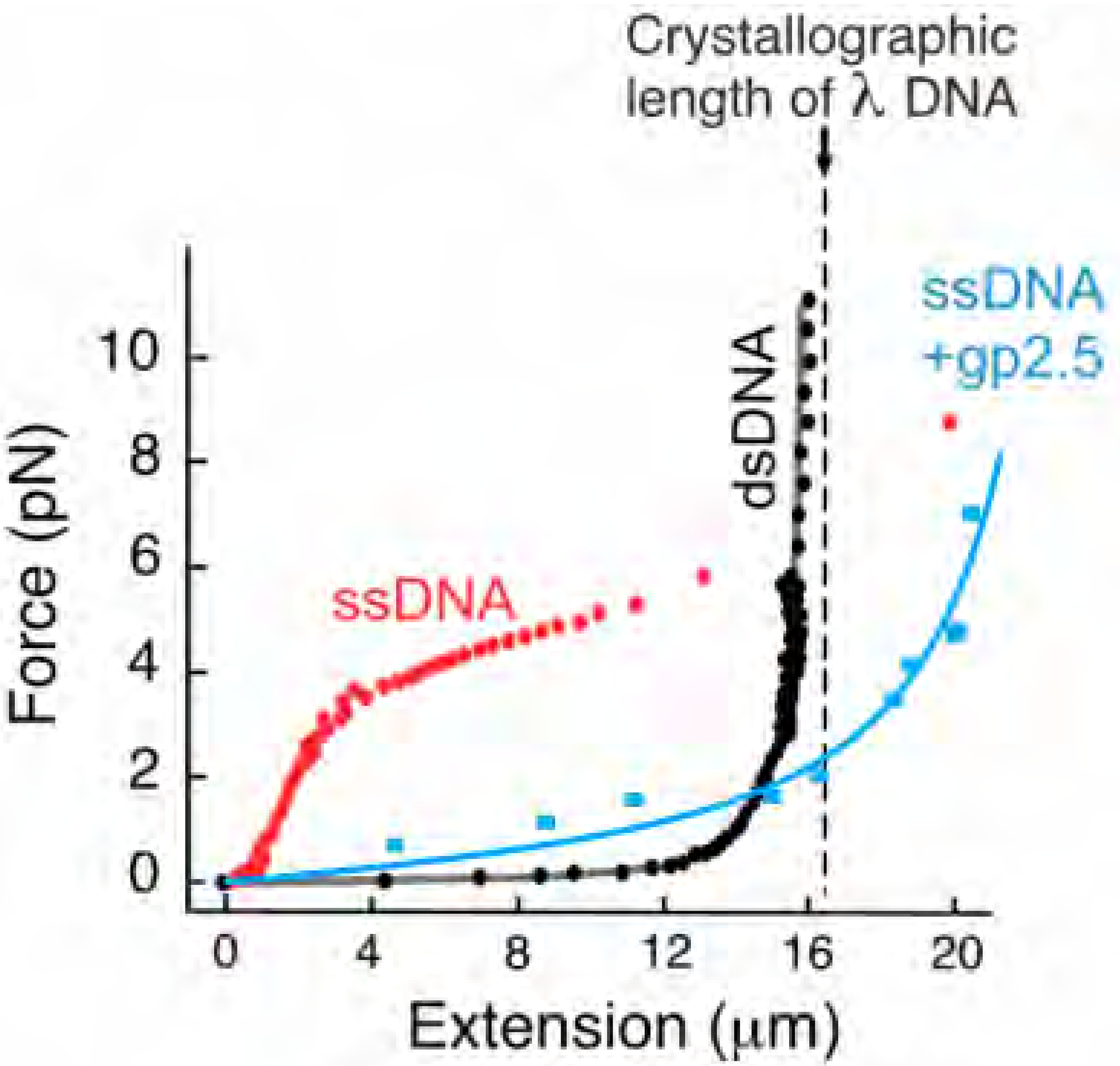
Crystallographic
length of λ DNA
ssDNA
+gp2.5
dsDNA
ssDNA
Force (pN)
0
2
4
6
8
10
0
4
8
12
16
20
Extension (μm)

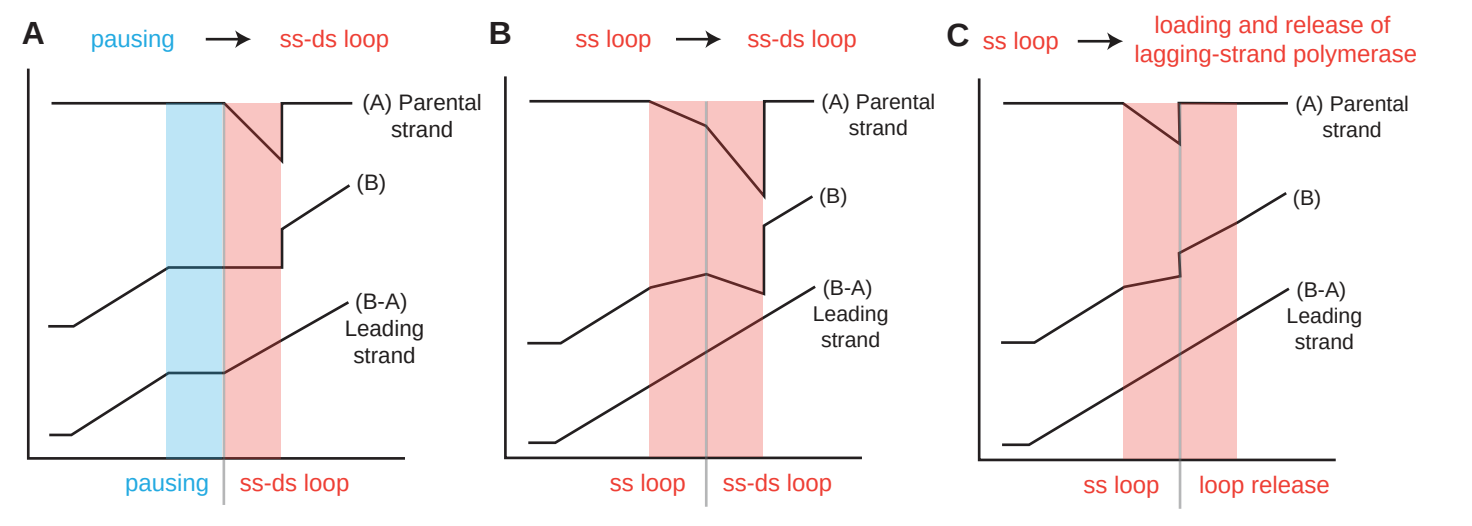
A
pausing
ss-ds loop
(A) Parental strand
(B)
(B-A) Leading strand
pausing
ss-ds loop
B
ss loop
ss-ds loop
(A) Parental strand
(B)
(B-A) Leading strand
ss loop
ss-ds loop
C
ss loop
loading and release of lagging-strand polymerase
(A) Parental strand
(B)
(B-A) Leading strand
ss loop
loop release

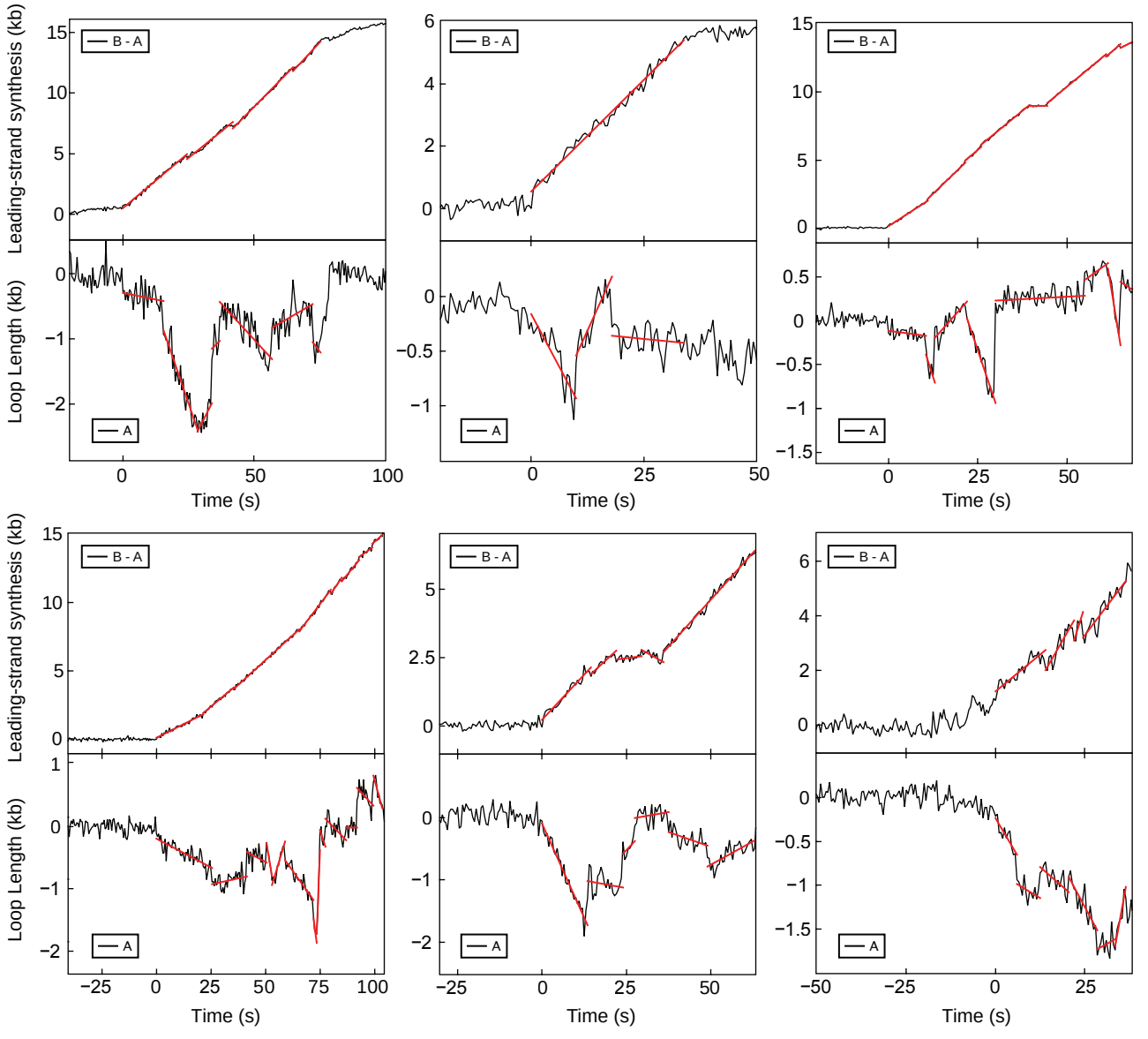
Leading-strand synthesis (kb)
Loop Length (kb)
B - A
A
Time (s)

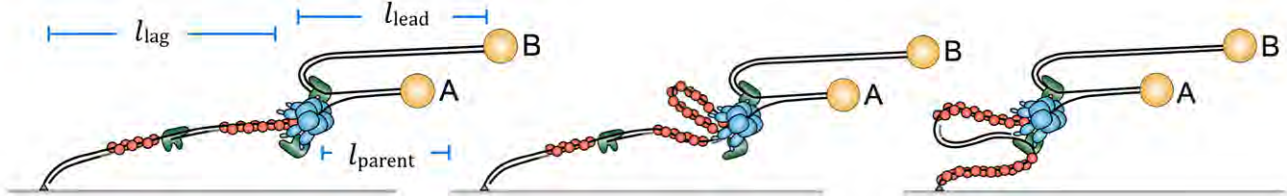

	Leading-strand synthesis only	ss loop	ss-ds loop
Bead A	$k_{lead} \cdot l_{lag} - k_{lead} \cdot l_{parent}$	$- k_{lead} \cdot l_{parent}$	$- k_{lead} \cdot l_{parent} - k_{lag} \cdot l_{lag}$
Bead B	$k_{lead} \cdot l_{lag} + k_{lead} \cdot l_{lead}$	$k_{lead} \cdot l_{lead}$	$k_{lead} \cdot l_{lead} - k_{lag} \cdot l_{lag}$
B - A	$k_{lead} \cdot l_{lead} + k_{lead} \cdot l_{parent}$	$k_{lead} \cdot l_{lead} + k_{lead} \cdot l_{parent}$	$k_{lead} \cdot l_{lead} + k_{lead} \cdot l_{parent}$

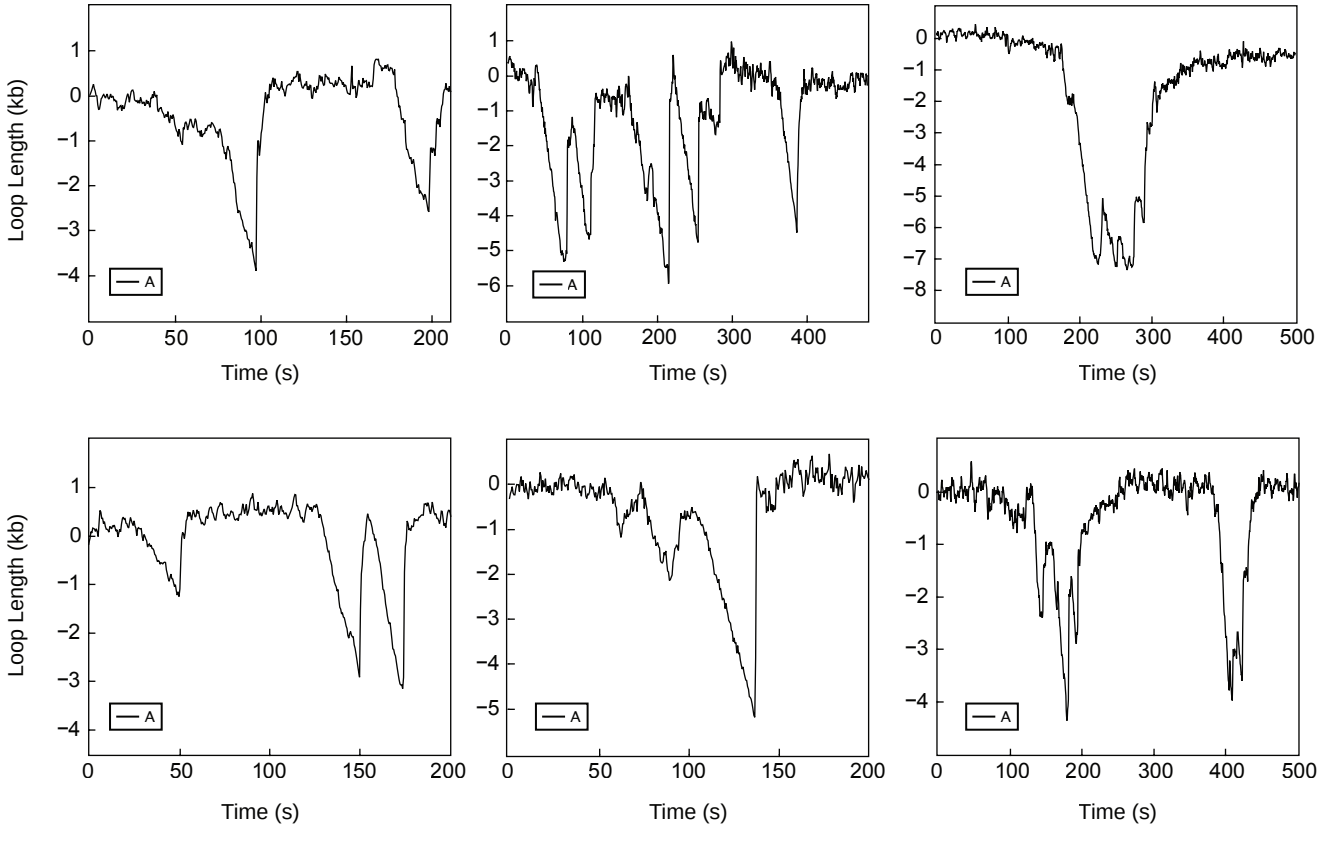
Loop Length (kb)
Time (s)
A
Loop Length (kb)
Time (s)
A

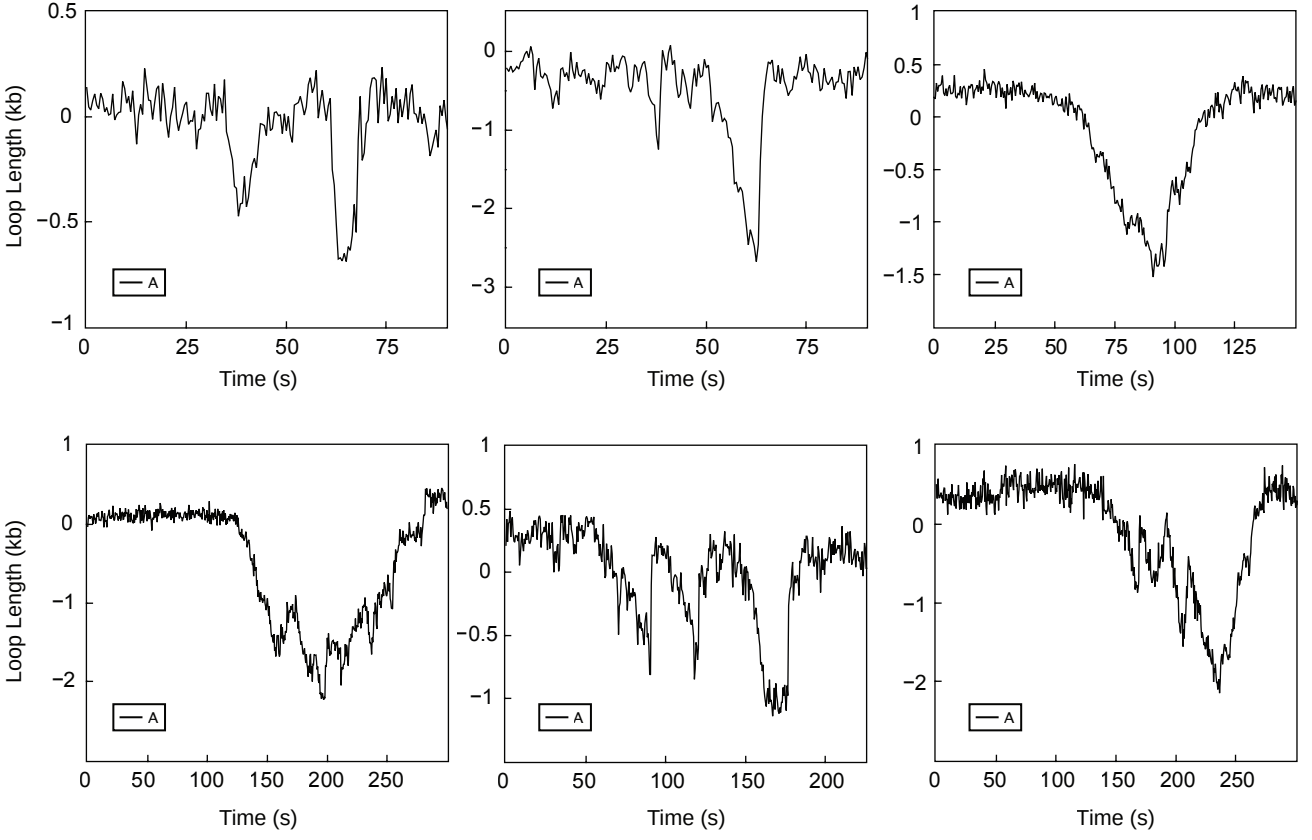
Loop Length (kb)
Time (s)
A
0.5
0
−0.5
−1
25
50
75
−2
−3
1
−1.5
100
125
150
200
250

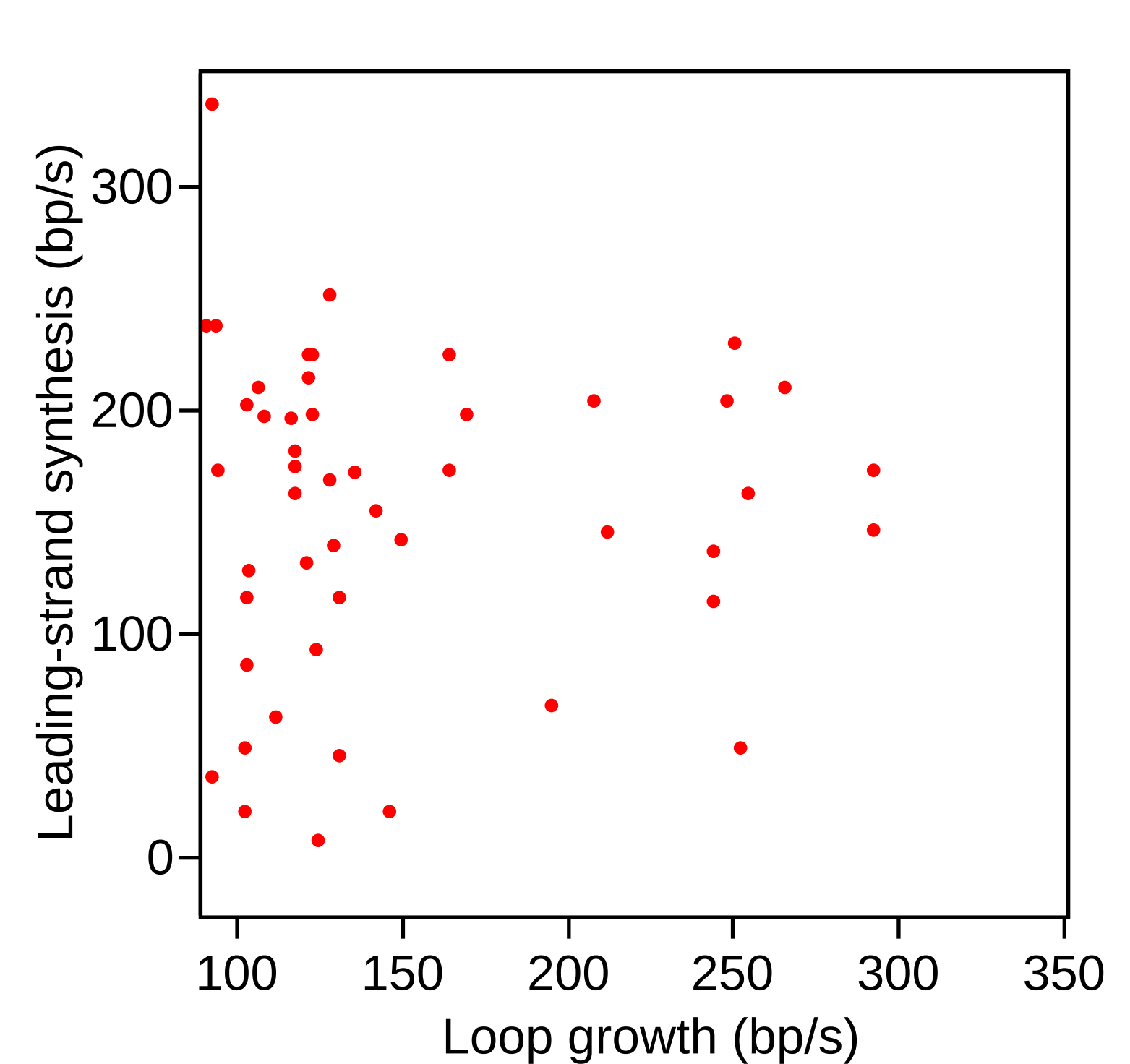
Leading-strand synthesis (bp/s)
300
200
100
0
100
150
200
250
300
350
Loop growth (bp/s)

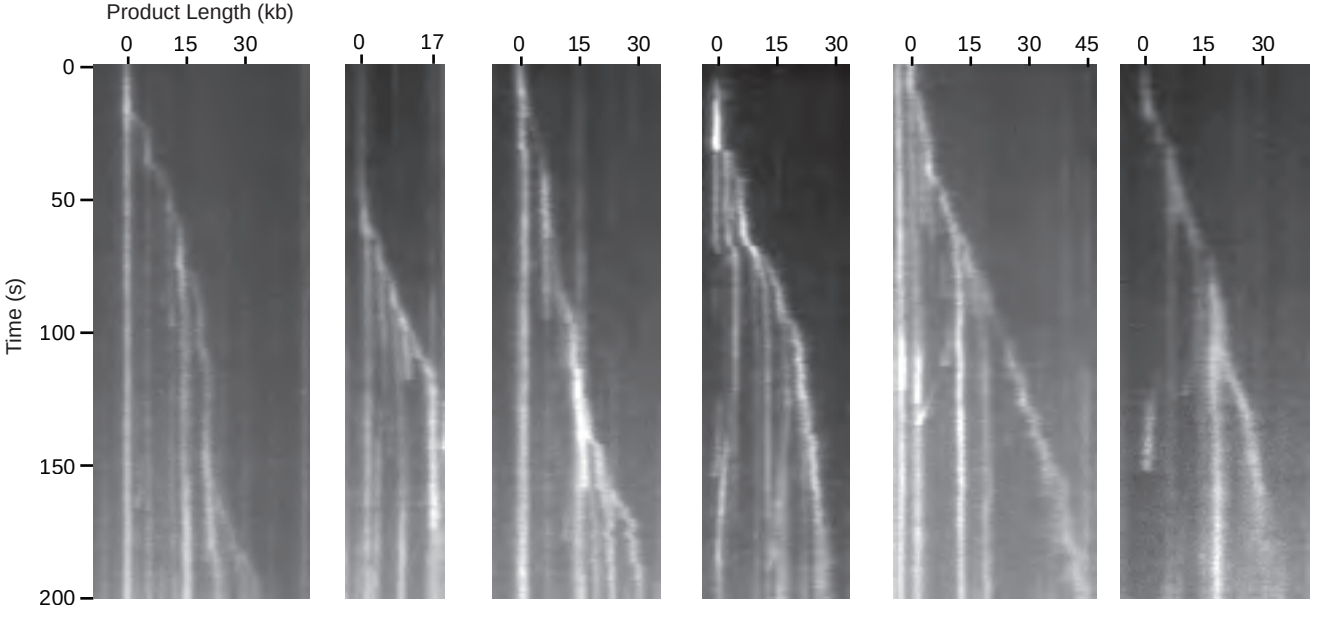
Product Length (kb)
0
15
30
0
17
0
15
30
0
15
30
0
15
30
45
0
15
30
Time (s)
0
50
100
150
200

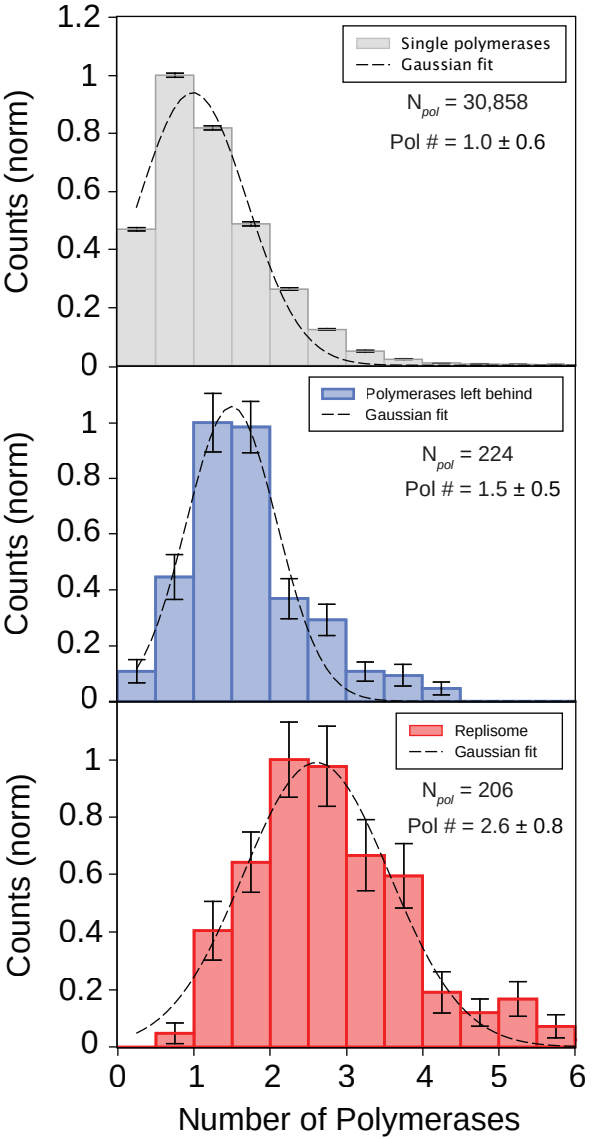
Single polymerases
Gaussian fit
N_pol = 30,858
Pol # = 1.0 ± 0.6
Polymerases left behind
Gaussian fit
N_pol = 224
Pol # = 1.5 ± 0.5
Replisome
Gaussian fit
N_pol = 206
Pol # = 2.6 ± 0.8
Counts (norm)
Number of Polymerases

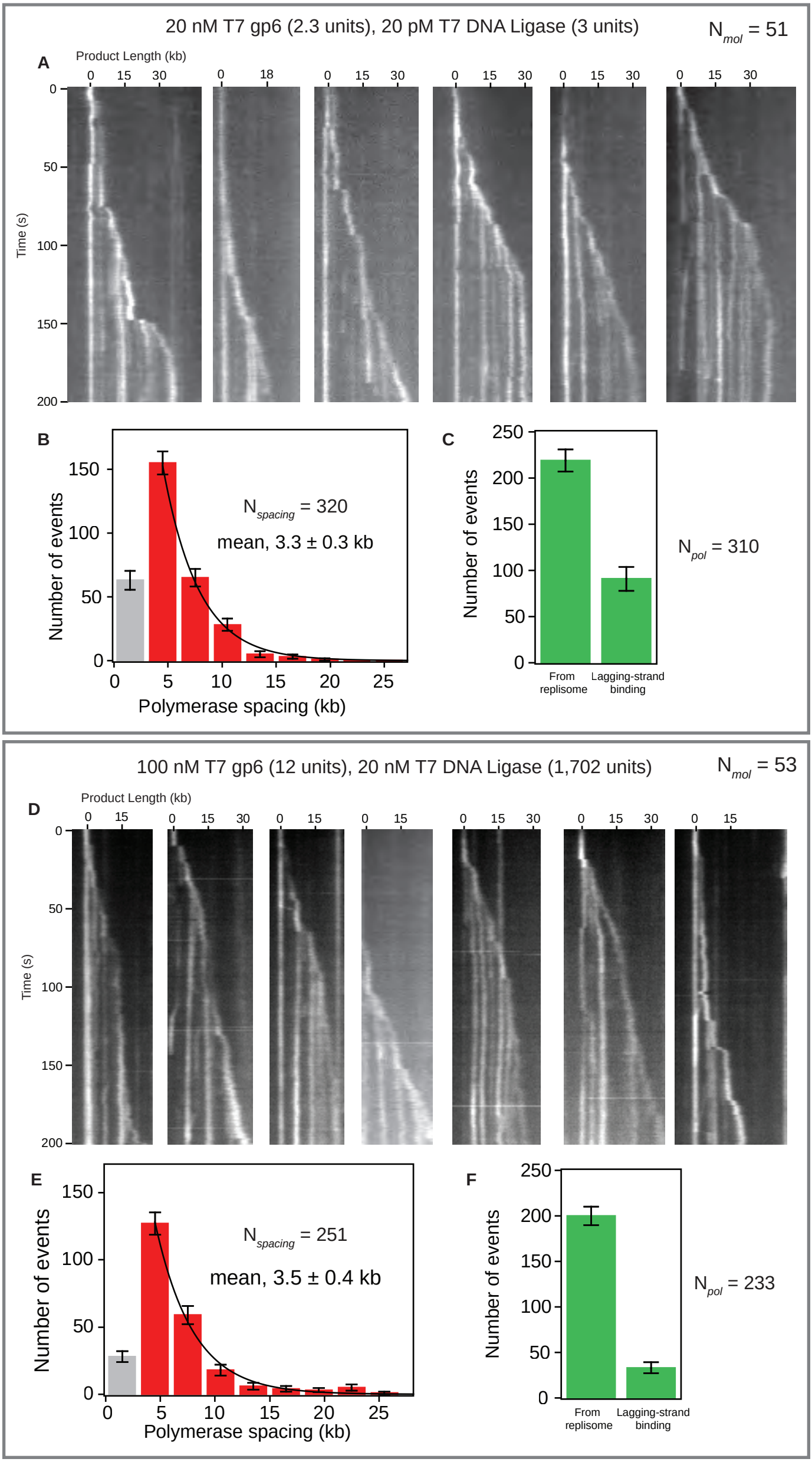
20 nM T7 gp6 (2.3 units), 20 pM T7 DNA Ligase (3 units)
N_mol = 51
A
Product Length (kb)
Time (s)
B
Number of events
N_spacing = 320
mean, 3.3 ± 0.3 kb
Polymerase spacing (kb)
C
Number of events
N_pol = 310
From replisome
Lagging-strand binding
100 nM T7 gp6 (12 units), 20 nM T7 DNA Ligase (1,702 units)
N_mol = 53
D
Product Length (kb)
Time (s)
E
Number of events
N_spacing = 251
mean, 3.5 ± 0.4 kb
Polymerase spacing (kb)
F
Number of events
N_pol = 233
From replisome
Lagging-strand binding

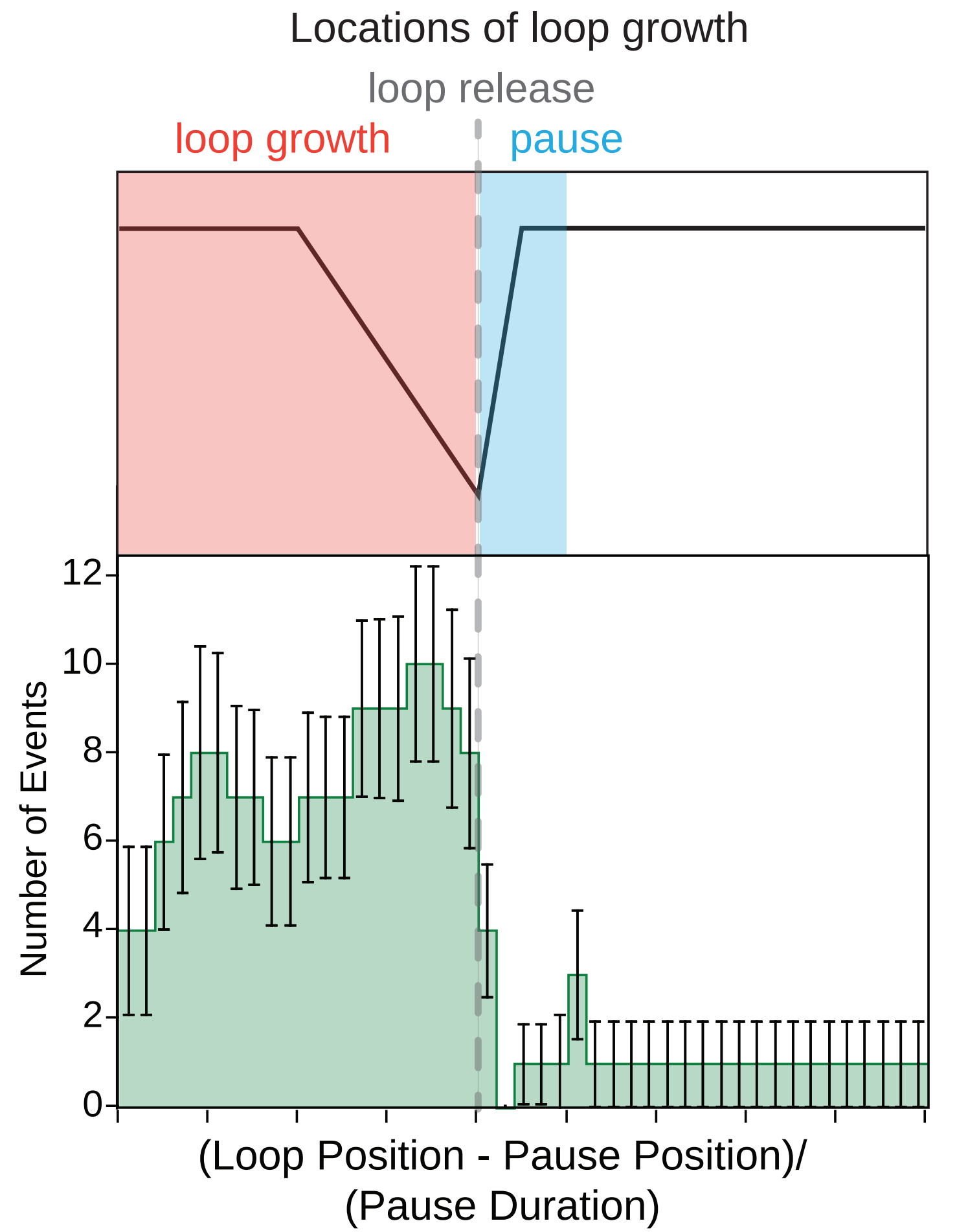
Locations of loop growth
loop release
loop growth
pause
12
10
8
6
4
2
0
Number of Events
(Loop Position - Pause Position)/
(Pause Duration)